T.C.
ÇANAKKALE ONSEKİZ MART UNIVERSITY
SCHOOL OF GRADUATE STUDIES

DEPARTMENT OF MOLECULAR BIOLOGY AND GENETICS.

ELUCIDATING THE ANTICANCER ACTIVITIES OF NOVEL TRIARYLBENZOPHENONE DERIVATIVES BY MECHANISM-BASED AND IN SILICO APPROACHES

MASTER OF SCIENCE THESIS

SERHAT DÖNMEZ

Thesis Supervisor
PROF. DR. TUĞBA TÜMER
Second Thesis Supervisor
ASSOC. PROF. MEHMET ÖZBİL

ÇANAKKALE – 2023

T.C.
ÇANAKKALE ONSEKİZ MART UNIVERSITY
SCHOOL OF GRADUATE STUDIES

DEPARTMENT OF MOLECULAR BIOLOGY AND GENETICS

ELUCIDATING THE ANTICANCER ACTIVITIES OF NOVEL TRIARYLBENZOPHENONE DERIVATIVES BY MECHANISM-BASED AND IN SILICO APPROACHES

MASTER OF SCIENCE THESIS

SERHAT DÖNMEZ

Thesis Supervisor
PROF.DR. TUĞBA TÜMER
Second Supervisor
ASSOC. PROF. MEHMET ÖZBİL

This study has been supported by the Scientific Research Project Coordination Unit of Türkiye 2210/C National MSc Scholarship Program and Çanakkale Onsekiz Mart University Scientific Research Project Coordination Unit
Project No: FIA-2021-3666 and FYL-2022-4122

ÇANAKKALE – 2023

T.C.
ÇANAKKALE ONSEKİZ MART ÜNİVERSİTESİ
LİSANSÜSTÜ EĞİTİM ENSTİTÜSÜ

The study entitled "**Elucidating the anticancer activities of novel triarylbenzophenone derivatives by mechanism-based and in silico approaches**" submitted by **Serhat DÖNMEZ** under the supervision of Prof. Dr. Tuğba TÜMER and second supervisor Assoc. Prof. Mehmet ÖZBİL was defended on **21/06/2023**. This thesis has been approved as **Master of Science in Molecular Biology and Genetics** of Çanakkale Onsekiz Mart University, School of Graduate Studies by the Examining Committee Members.

Examining Committee	**Signature**
Prof. Dr. Tuğba TÜMER (Supervisor)	……
Prof. Dr. Kemal Melih TAŞKIN (Member)	……
Prof. Dr. Feray KÖÇKAR (Member)	……

Tez No : 10545113
Tez Savunma Tarihi : 21/06/2023

……
Prof. Dr. Ahmet Evren ERGİNAL
Director
School of Graduate Studies

PLAGIARISM DECLARATION

Çanakkale Onsekiz Mart Üniversitesi Lisansüstü Eğitim Enstitüsü Tez Yazım Yönergesi'ne uygun olarak hazırladığım bu tez çalışmasında; tez içinde sunduğum verileri, bilgileri ve dokümanları akademik ve etik kurallar çerçevesinde elde ettiğimi, tüm bilgi, belge, değerlendirme ve sonuçları bilimsel etik ve ahlak kurallarına uygun olarak sunduğumu, tez çalışmasında yararlandığım eserlerin tümüne uygun atıfta bulunarak kaynak gösterdiğimi, kullanılan verilerde herhangi bir değişiklik yapmadığımı, bu tezde sunduğum çalışmanın özgün olduğunu, bildirir, aksi bir durumda aleyhime doğabilecek tüm hak kayıplarını kabullendiğimi taahhüt ve beyan ederim.

I declare that all the information and results offered in visual, and written from are obtained by myself observing the academic and ethical rules. Moreover, all other results and information referred to in the thesis but not specific to this study are cited.

Serhat DÖNMEZ
21/06/2023

ACKNOWLEDGEMENTS

Firstly, I would like to express my deepest gratitude to my supervisor, Prof. Dr. Tuğba TÜMER, for her invaluable support, unwavering motivation, and endless patience. She shared her knowledge throughout my study and gave me a role in many scientific projects. Her guidance and mentorship improved my scientific and academic skills. Also, her motivation and scientific perspective is a source of inspiration for me.

I would like to extend my sincere thanks to my second supervisor Assoc. Prof. Mehmet ÖZBİL, for teaching me computational-based analyses and teaching me to think like a computational biochemist, for sharing his knowledge, and for his support and motivation.

I especially thank to Berkay and Özlem for teaching me everything I know about working in a cell culture laboratory. Also, I would like to thank my labmate Hazal, newcomers İlknur, Melek, and Oğuzhan, and my dear friends, Kübra, Raşit, and Taylan for sharing all the joy, tears and laughters together all through the years. I consider myself incredibly fortunate to have friends like you by my side.

Words cannot express my gratitude to my mom Bedia DÖNMEZ and my dad Selvet DÖNMEZ for their constant encouragement and belief in my abilities. This journey would not have been possible without them.

Finally, I wish to acknowledge the financial support given by COMU Scientific Research Projects Coordination Unit (Project No: FYL-2022-4122). I am also thankful to the National MSc Scholarship Program (Program code: 2210-C) granted by Scientific Research Project Coordination Unit of Türkiye (TUBITAK) and TUBITAK ULAKBIM for allowing me to access High Performance and Grid Computing Center (TRUBA resources).

Serhat DÖNMEZ

Çanakkale, June 2023

ÖZET

ÖZGÜN TRİARİLBENZOFENON TÜREVLERİNİN ANTİKANSER AKTİVİTELERİNİN MEKANİZMA-BAZLI VE İN SİLİCO YAKLAŞIMLARLA AYDINLATILMASI

Serhat DÖNMEZ
Çanakkale Onsekiz Mart Üniversitesi
Lisansüstü Eğitim Enstitüsü
Moleküler Biyoloji ve Genetik Anabilim Dalı Yüksek Lisans Tezi
Danışman: Prof. Dr. Tuğba TÜMER
İkinci Danışman: Doç. Dr. Mehmet ÖZBİL
20/06/2023, 48

Son zamanlarda çok hedefli ilaçların geliştirilmesi kanser tedavisinde kullanılan stratejilerden biridir. Bu strateji, ilaçların etki gücünü arttırmakla beraber istenmeyen yan etkileri de azaltmaktadır. Bu çalışmada, özgün triarilbenzofenon türevlerinin antikanser aktiviteleri ve dual (ikili) topoizomeraz I/II inhibisyon kapasitelerini in vitro ve in silico teknikleri kullanarak araştırılmıştır. Bulgulara göre, özellikle **SMR-36** bileşiği prostat ve kolon kanseri hücrelerinin hücre canlılığını, göç ve koloni oluşturma kabiliyetlerini seçici olarak inhibe ederken sağlıklı hücreler üzerinde minimum sitotoksik etkinlik göstermiştir. Ayrıca, triarilbenzofenon türevleri hem topoizomeraz I hem de topoizomeraz II enzim aktivitesini yüksek bir etkinlikle inhibe etmiştir. Enzim inhibisyon deneylerinden elde edilen bulgularla benzer şekilde in siliko moleküler kenetlenme ve dinamik simülasyonları çalışmalarında da bileşiklerin topoizomerazların katalitik bölgesine karşı yüksek bağlanma afinitesi gösterdiği yönünde bulgular elde edilmiştir.

Sonuç olarak, triarilbenzofenon türevlerinin ikili topoizomeraz inhibitörleri olarak kanser tedavisinde kullanılmak üzere umut vadeden bir potansiyeline sahip olabilir ve bu bileşikler etkinlikleri arttırılacak şekilde geliştirilebilir.

Anahtar Kelimeler: Kanser, İkili inhibisyon, İn siliko moleküler kenetlenme, İn vitro, Topoizomeraz

ABSTRACT

ELUCIDATING THE ANTICANCER ACTIVITIES OF NOVEL TRIARYLBENZOPHENONE DERIVATIVES BY MECHANISM-BASED AND IN SILICO APPROACHES

Serhat DÖNMEZ

Çanakkale Onsekiz Mart University

School of Graduate Studies

Master of Science Thesis in Molecular Biology and Genetics

Supervisor: Prof. Dr. Tuğba TÜMER

Co-supervisor: Assoc. Prof. Mehmet ÖZBİL

20/06/2023, 48

Multitargeted drug development represents a novel approach in the field of cancer treatment. By employing this strategy, the efficacy of drugs can be enhanced while concurrently minimizing undesired side effects. This study aims to evaluate anticancer activities and dual topoisomerase I/II inhibition capacities of novel triarylbenzophenone derivatives by using in vitro and in silico techniques. The results demonstrated that **SMR-36** selectively inhibited the survival, migration, and colony formation capabilities of prostate and colon cancer cell lines, while exhibiting minimal effects on healthy cells. Additionally, the triarylbenzophenone derivatives showed inhibitory effects on both topoisomerases I and II enzyme activity. Consistent with the findings from enzyme inhibition assays, in silico molecular docking and dynamics studies revealed that the compounds yielded high binding affinity towards the catalytic site of the topoisomerases.

To summarize, the findings suggest that triarylbenzophenone derivatives possess the potential to serve as dual topoisomerase inhibitors and can be further developed as promising candidate anticancer agents.

Keywords: Cancer, Dual inhibition, in silico molecular docking, in vitro, Topoisomerase

TABLE OF CONTENT

Page No.

ABBREVIATIONS

DMEM	Dulbecco's Modified Eagle Medium
°C	Degree Celsius
DMSO	Dimethyl Sulfoxide
DOX	Doxorubicin
FBS	Fetal Bovine Serum
HT-29	Human Colon Cancer Cell Line
HUVEC	Human Healthy Endothelial Cell Line
IC_{50}	Half Maximal Inhibitory Concentration
MCF-7	Human Breast Cancer Cell Line
PBS	Phosphate-Buffered Saline
PC-3	Human Prostate Cancer Cell Line
SRB	Sulforhodamine B
µg	Microgram
µl	Microliter
FDA	Food and Drug Administration
SPC	Simple Point Charge
TOPO I	Topoisomerase I
TOPO II	Topoisomerase II
U	Units of Enzyme
RMSD	Root-mean-square deviation

LIST OF TABLES

LIST OF FIGURES

CHAPTER 1
INTRODUCTION

Cancer is one of the most deadly diseases afflicting humans. According to the World Health Organisation (WHO), in 2021, almost 18 million people lost their lives because of cancer and this number is expected to increase 2 fold in 2040. Among all of the cancer types, the most lethal ones are breast, colorectum and prostate cancer. These cancer types form 30 % of all cancer cases (Ferlay et al., 2021). Due to possible expectations in the number of cases, there is a need for new anticancer agents and therapeutic approaches.

There are different types of anticancer agents used for cancer treatment. For example, alkylating agents, such as cyclophosphamide, and chlorambucil which cause damage the DNA of the cancerous cells and prevent their proliferation (Emadi et al., 2009). Agents like antimetabolites such as 5-fluorouracil, and cytarabine. These drugs mimic the building blocks of DNA and RNA, thus, preventing the cancer cells from dividing and spreading by replacing the original bases. Another type of anticancer agent includes topoisomerase inhibitors, which can interfere with the division of cancer cells by targeting the enzymes involved in DNA replication and mitotic inhibitors. Nowadays, anticancer agent development focuses more on targeting multiple biological molecules with one compound. This approach is increasing the anticancer effect of the compounds while decreasing the side effects. One of the well-known approach is the dual topoisomerase I (TOPO I) and II (TOPO II) inhibition (Nitiss, 2009).

1.1. Topoisomerase inhibitors

DNA molecules can be found in different forms in the cells such as superhelix, catena and knot. Also, during DNA replication, the opening of DNA strands causes the formation of supercoiled DNA structures. These forms of the DNA create obstacles both for the replication and transcription processes. To overcome this problem, topoisomerase enzymes bind to the DNA and generate short temporary breaks (Figure 1). The breaks cause the

formation of different topological forms such as relaxation, and catenation/decatenation without changing the DNA structure. By this way, DNA replication or transcription processes can be completed without any errors or damage. Two types of topoisomerase are present in the cell; Type I and Type II. Type I class enzymes create DNA single-strand breaks, while, Type II class enzymes are responsible for the decatenation, as they cause double-strand breaks on the DNA molecule (Nitiss, 2009).

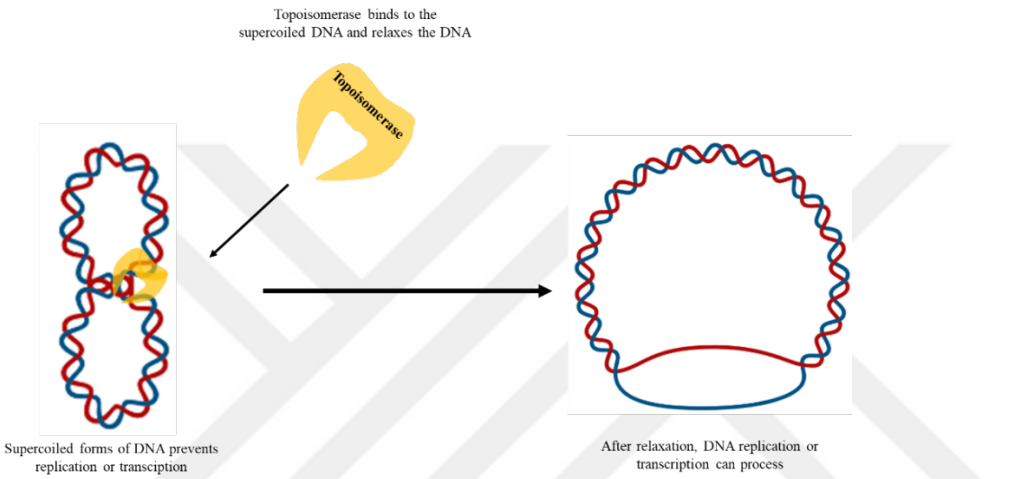

Figure 1. Simple presentation of topoisomerase enzyme activity.

Topoisomerase enzymes also play a vital role in DNA transcription and gene regulation. For example, the RNA polymerase creates positive superhelical structures in front of the transcription bubble and negative superhelical structures behind the bubble. If supercoiled structures are not regulated, they can cause problematic alterations in the transcription process. In addition, folded DNA structures are more likely to form stable DNA-RNA hybrids (R-loop) than relaxed double strands. These structures inhibit cell growth and cause genomic instability by increasing transcription levels (Vos et al., 2011).

Due to their important role in both replication and transcription systems, topoisomerases are associated with cell growth and proliferation. Furthermore, elevated topoisomerase expression enables cancer cells to proliferate faster than healthy cells. For

above-mentioned reasons, inhibition of topoisomerase enzymes is considered as promising therapeutic approach for the prevention of cancer cell development (Vos et al., 2011).

1.1.1. Anticancer activity of topoisomerase I (TOPO I) inhibitors

There are various FDA-approved topoisomerase inhibitor drugs available on the market. Among all of the drugs, the most well-known ones are camptothecin and its derivatives (Figure 2). Camptothecin is firstly isolated from the *Camptotheca acuminate* plant. Studies showed that the compound effective against melanoma, colon and gastrointestinal cancer cells in both cell-based and clinical studies. In the 1980s, both camptothecin usage and topoisomerase inhibition drew massive attention and studies indicated that Camptothecin selectively inhibits the TOPO I enzyme activity by interacting with the topoisomerase I/DNA complex, thus stabilizing the structure. The promising effects of Camptothecin on cancer treatment lead to the development of new and more effective drugs (Martino et al., 2017).

Topotecan and irinotecan are also FDA-approved semi-synthetic derivatives of camptothecin. Topotecan is highly soluble in water compared to camptothecin and is generally used for the treatment of ovarian cancer patients who have resistance to platinum-based drug treatments such as cisplatin and carboplatin. Clinical trials of topotecan suggested that it can also be used for the treatment of colon, lung, and bone cancers. Similarly, irinotecan was found effective on colon, lung, breast, and ovarian cancer at cell-based assays and clinical levels (de Man et al., 2018).

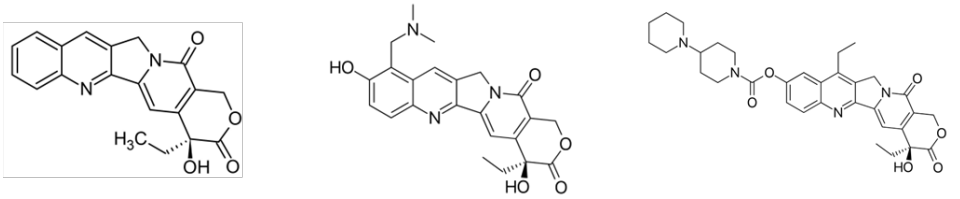

Figure 2. 2D structure of FDA approved topoisomerase I inhibitors

Topoven, LMP744, LMP776, and LMP400 are not camptothecin derivatives, however, the action mechanism of these compounds was similar to the camptothecin except for binding to different DNA sides, which could result in various cellular effects. They are more stable and bind to TOPO I more irreversible compared to camptothecin. Furthermore, Topoven (also known as ARC-111) was shown to inhibit tumour formation colon cancer xenography model and inhibit cell proliferation of colon cancer, leukaemia and lymphoma cell lines with IC_{50} values ranging from 0.002 to 1.43 μM. Clinical studies of Topoven still continues and, LMP744, LMP776 and LMP400 compounds are currently under phase I clinical trial on patients with lymphoma (Li et al., 2003).

1.1.2. Anticancer activity of topoisomerase II (TOPO II) inhibitors

TOPO II inhibitors can disrupt TOPO II activity by binding to the DNA or the ATP molecule, thus, increasing ATP hydrolysis or DNA cleavage. Inhibitors may have very distinct cellular effects depending on the action mechanism (Okoro & Fatoki, 2023). Accordingly, TOPO II inhibitors are classified into two types. (Figure 3).

Catalytic topoisomerase II inhibitors

Catalytic TOPO II inhibitors bind to the TOPO II and stabilize TOPO II–DNA complexes. Aclarubicin and Suramin are examples of known catalytic TOPO II inhibitors. Aclarubicin causes cell cycle arrest at the S phase in cancer cells due to its strong inhibitory

activity and is used for the treatment of leukaemia. On the other hand, Suramin is used for the treatment of prostate and brain cancer and inhibits TOPO II. (IC_{50} value of 5 µM) (Grossman et al., 2001).

Topoisomerase II poisons

TOPO II poisons form a complex with TOPO II and stabilize the enzyme-DNA complex and the formation of DNA double-strand breaks, unlike catalytic inhibitors. The most known TOPO II poisons are etoposide and doxorubicin. The FDA authorized etoposide in 1983, and it is still used to treat lung, blood, prostate, and breast cancers. Doxorubicin was approved by FDA in the middle of the 1970s and is still used for the treatment of several cancers including breast, lung, gastric, and ovarian. Doxorubicin inhibits the TOPO II DNA ligation activity similar to etoposide, but significantly low doses (<1 µM) than etoposide (Fisher & Pan, 2008).

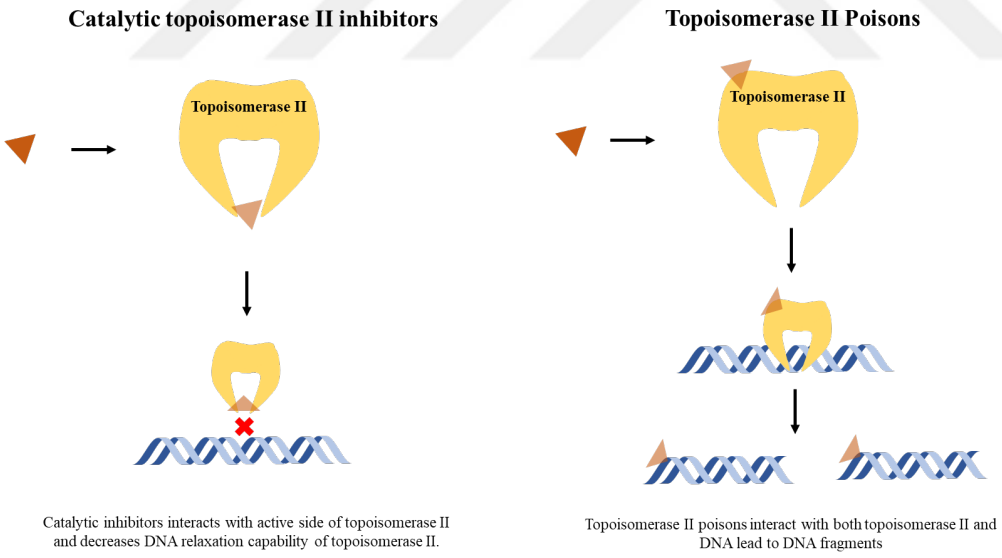

Figure 3. Action mechanism of topoisomerase II catalytic inhibitors and poisons.

1.1.3. Dual Topoisomerase I/II Inhibitors

Topoisomerase inhibitors have promising anticancer effects on various cancer cells as described above. However, usage of selective TOPO I inhibition may lead to increases in the activity of TOPO II or vice versa. Regarding this, it was proposed that drug resistance to one type of topoisomerase inhibitor may be altered by using an inhibitor of another type. For instance, usage of topotecan (a kind of TOPO I inhibitor) increased the expression level of TOPO II in chronic myelogenous leukaemia (CML) and colon cancer cells and increased the sensitivity of the cells to topoisomerase II inhibitor (etoposide) (Chen et al., 2002). In this situation, TOPO II has emerged as a new anticancer target. Accordingly, dual inhibition of TOPO I and II could be beneficial to overcome this vice versa increase in activity of topoisomerases thus drug resistance. Besides, the use of dual inhibitors at low doses may alter undesired side effects of selective TOPO I or II inhibitors such as headache, dizziness and cardiovascular toxicity. Currently, there are dual topoisomerase inhibitors that have passed into the clinical trial phases such as TAS-103, Tafluposide, and elomotecan (Figure 4). Another dual inhibitor is the TAS-103 molecule which inhibits both TOPO I and TOPO II enzymes effectively with IC_{50} values of 2 and 6.5 μM, respectively (Denny & Baguley, 2005). Tafluposide, also known as F 11782, is a derivative of etoposide with dual catalytic inhibition of TOPO I/II. Tafluposide has exhibited a promising anticancer effect on in vivo breast, leukaemia, and lung xenograft models. Elomotecan, also known as (BN80927), was derived from the camptothecin and similar to the parent molecule's activity on TOPO I, while, also having a catalytic inhibitory activity on TOPO II. Also, elomotecan has strong activities against in vitro and in vivo colon, prostate, ovary lung and breast cancer models. Phase I clinical trials with the compound are ongoing. Also, phase II clinical studies with TAS-103 on small-lung cancer treatment are ongoing (Skok et al., 2020).

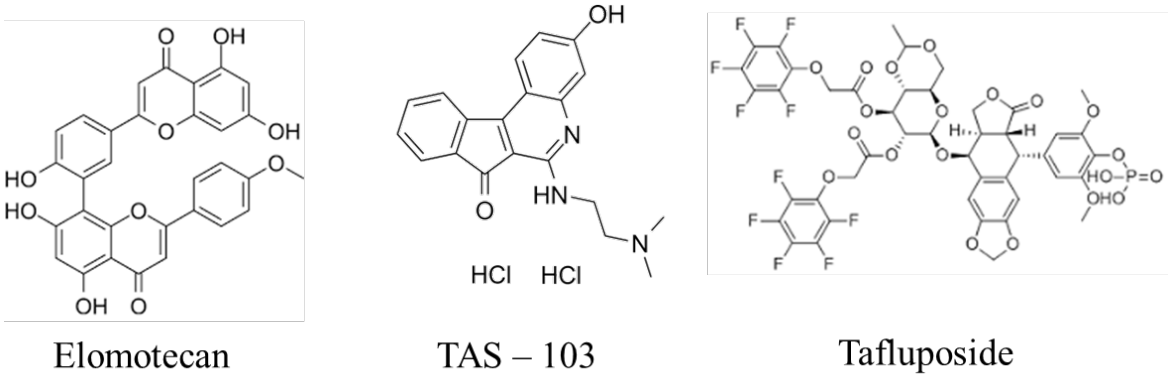

Figure 4. 2D structure of dual TOPO I and II inhibitors.

1.2. Triarylbenzophenones

The triarylbenzophenone derivatives have a structure composed of 4-hydroxy/methoxy phenyl and 3,4,5-trisubstituted phenyl rings attached to the carbonyl group. Also, most of the triarylbenzophenone derivatives were evaluated from *Selaginella*. The plant was used in traditional Chinese medicine for the treatment of numerous disorders such as jaundice, gonorrhoea, hemorrhage, and severe hepatitis. In 2014, the first triarylbenzophenone-based compounds were isolated, characterized and then synthesized by organic chemistry methods from *Selaginella*. In the same study, it was shown that the compounds inhibited cell viability of coxsackie virus B3 (CVB3) infected human laryngeal carcinoma (HEp-2) cells with IC_{50} values ranging from 16-25 µg/mL. Furthermore, the administration of the compounds increased the survival rate of virus-infected mice by almost 80 % (Yin et al., 2014). In another study, enzyme-based tests were used to assess the effect of the substances on the PDE4D2 enzyme. According to the findings, the compounds inhibited the PDE4D2 enzyme with high efficiency (with an IC_{50} value ranging from 0.11 to 0.26 µM) (X. Liu et al., 2014). The aforementioned findings have heightened interest in the production of novel triarylbenzophenone-based molecules from the *Selaginella* and the derivatisation of already synthesized compounds with pharmacophore-based models and, recently, studies showed that triarylbenzophenone derivatives utilized cytotoxicity on prostate, breast, colon and liver cancer cells.

1.3 Aim of the thesis

This thesis aims to evaluate the anticancer, anti-proliferative effect of novel triarylbenzophenone derivatives through in vitro and in silico analyses. Synthesis of triarylbenzophenone derivatives were conducted by Dr. Lucas Rycek from Charles University (Czech) (Figure 5). As mentioned in the previous section triarylbenzophenone derivatives have a promising anticancer effect on cancer cell lines. Furthermore, the benzene, hydroxyl (-OH) and methoxy (-OMe) group rich content of the compounds were similar to the topoisomerase inhibitors. In light of this information, novel triarylbenzophenone derivatives were screened on breast, colon and prostate cancer cell lines through in vitro assays for the first time. Additionally, TOPO I and TOPO II inhibition experiments were also carried out to investigate the topoisomerase inhibitory capability of the compounds. Molecular docking and molecular dynamics, simulations were performed under the supervision of Assoc. Prof. Dr. Mehmet Özbil.

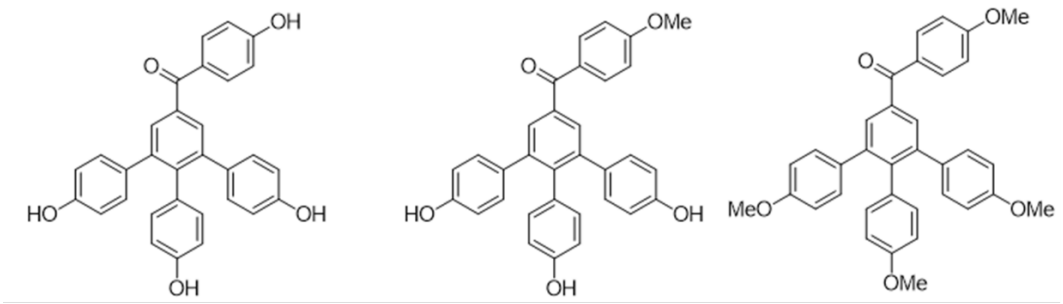

Figure 5. 2D structure of novel triarylbenzophenone derivatives.

Taken all together, in this thesis study;

- Cytotoxic effect of all compounds on the aforementioned cell lines was clarified by SRB assay.

- Cell cycle, apoptosis and qPCR analyses were performed by lead compounds to determine the effect of lead compounds on cell death.

- Topoisomerase inhibition effect of the compounds were clarifed by performing in vitro enzymatic assays and molecular docking and dynamics simulations.

CHAPTER 2
PREVIOUS STUDIES

Triarylbenzophenone derivatives used in this study (SBB, SMR36, SMR32-2) were not studied in the scope of any scientific research project. Further, no study showed the inhibitory impact of the compounds on the TOPO I/II enzyme. However, studies reveal the anticancer effects of triarylbenzophenone derivatives which are also different from the compounds handled in the current work, synthesized from the *Selaginella* plant. To summarize them,

Six distinct triarylbenzophenone compounds were obtained from the ethanol extract of *Selaginella Pulvinata* and the compounds were investigated for their inhibitory effect on the phosphodiesterase 4D (PDE4D) enzyme family. Accordingly, the compounds inhibited the enzyme activity of the PDE4D2 enzyme effectively. Among the compounds 2 and 5 showed the highest potent inhibitory effect (IC_{50} value of 1.04 and 1.25 μM) (X. Liu et al., 2018).

In a separate study conducted by the same research group, a different triarylbenzophenone analog was synthesized from the *Selaginella tamariscina* (species of *Selaginella*). Then, the cytotoxic effect of the compound was determined on two hepatocellular carcinoma cell lines. According to the results, the triarylbenzophenone derivative was decreased the cell viability of the cancer cells with IC_{50} values of 39.8 and 51.5 μM, respectively (R. Liu et al., 2020).

C. G. Wang et al., 2018 synthesized a triarylbenzophenones from the *Selaginella tamariscina*. Then, the compound was screened on lung, bladder and liver cancer cell lines. Results indicated that the compound did not show any cytotoxic effect even at the highest dose of application (>50 μM). Furthermore, the effect of the compound on the matrix metalloproteinases (MMPs) enzyme family was investigated by ex vivo enzyme assay. Triarylbenzophenone derivative inhibited MMP-2, and MMP-3 enzyme activity with IC_{50}

values 54.2, 66.1 μM. On the other hand, the compound did not inhibit MMP-9 enzyme activity (Wang et al., 2018).

Recently, Lapinskaite et al. (2023) investigated the anticancer and antimicrobial effect of newly synthesized triarylbenzophenone-based compounds. Firstly, the effect of the compounds on the PDE4 enzyme was utilized by measuring cyclic adenosine monophosphate (cAMP) release in HEK293 (human embryonic kidney cell line) cells. Results showed that none of the compounds inhibited cAMP release thus PDE4 enzymatic activity. This outcome was unexpected due to the previously reported PDE4 inhibitory effect of triarylbenzophenone derivatives. Further, the cytotoxic effect of these compounds was screened on three different cancer and healthy cell lines. The compounds showed a weak cytotoxic effect on the MCF-7 cell line, while, they showed a moderate cytotoxic effect on colon and prostate cancer cell lines Among the compounds, 4ca utilized the highest potent cytotoxic effect across the HT-29 and PC3 cell lines (IC_{50} value of 11.9 and 7.8 μM respectively). Also, compound 4ba showed the highest selectivity score towards the HT-29 cell line (8.2). In addition to cytotoxicity studies, the compounds were also tested for antibacterial activity on three distinct bacterial strands and none of these compounds showed any antimicrobial effect (Lapinskaite et al., 2023).

In conclusion, triarylbenzophenones synthesized from the different species of the *Selaginella* plant have an anticancer effect on various cancer cell lines. Even though most of the synthesized compounds were found effective on the PDE4 enzyme family, the compounds can target other biological molecules such as the MMP enzyme family. Also, due to the structural similarity of the compounds with topoisomerase inhibitors, we thought that the compounds might target topoisomerases.

CHAPTER 3
MATERIALS AND METHODS

3.1. Materials

3.1.1. Chemicals and Kits

All reagents used in this study were listed below (Table 1).

Table 1

List of reagents used in this study.

Chemicals and Kits	Brand - Catalogue Number
Methanol	Sigma-Aldrich Chemical - 24229
Acetic Acid	Sigma-Aldrich Chemical - 1.00056.2500
Trypan blue solution	Sigma-Aldrich Chemical - T6146
Sodium pyruvate	Sigma-Aldrich Chemical - P5280
Dimethyl sulfoxide (DMSO)	Sigma-Aldrich Chemical - D2650
Sulforhodamine B sodium salt	Sigma-Aldrich Chemical - S 1402
Doxorubicin hydrochloride	Sigma-Aldrich Chemical - D2975000
L-Cysteine	Sigma-Aldrich Chemical - C7352
Trisma base	Sigma-Aldrich Chemical - T1503
Crystal Violet	Sigma-Aldrich Chemical - 548 62 9
Dulbecco's Modified Eagle's Medium (DMEM)	Life Technolo ies Thermo Fisher Scientific - 12800017
Trypsin-EDTA	Life Technolo ies Thermo Fisher Scientific - 25200056
Fetal bovine serum (FBS)	Life Technolo ies Thermo Fisher Scientific - 10500064
Penicillin-streptomycin	Life Technolo ies Thermo Fisher Scientific - 15140122
Dimeth 1 sulfoxide (DMSO)	Santa Cruz Biotechnology - sc-358801
Dulbecco's PBS	Caisson laboratories - PBPOI
Human Topoisomerase I Assay Kit	TOPOGEN - TG1015-3A
Human Topoisomerase II Assay Kit	TOPOGEN - TG1001-3A
RedSafe Nucleic Acid Staining Solution	iNtRON - 21141
EDTA	BioShop Canada Inc.- EDT002.500

3.1.2. Equipment

All of the devices and equipment used in this study were listed below (Table 2).

Table 2

List of devices and equipment used in this study.

Brand - Model	Equipment
BUCHI - V 300	Vacuum pump
Esco - CCL 170T 8	Cell culture CO2 incubator
Esco - Class II BSC	Biological safety cabinet
Hettich - Universal 320R	Standard centrifuge
Hettich - MIKRO 200R	Refrigerated Micro Centrifuge
TECAN - Infinite 200 PRO	Microplate reader
Scientific Industries - Genie 2	Vortex
Invitrogen - Qubit 4	Flurometer
HANNA Instruments - HI 2211	pH meter
Thermof Fisher Scientific - Applied BiosystemsTM 7500	Real-Time PCR Systems
Bio-Rad - PowerPacTM Basic	Basic Power Supply
Cleaver Scientific - MS 120910874	Wide Midi Horizontal Electrophoresis System
Vilber Lourmat - QUATUM ST4 1100 26MX	Gel Documentation Imaging System
Bio-Rad - T100TM	Thermal Cycler
Beckman Coulter - Allegra X-15R	Refrigerated Centrifuge

3.1.3. Cell Lines

Cancer and healthy cell lines used for this study and their growth medium were listed below. Cells were maintained at 37 ℃ in humidified air containing 5 % CO_2. Cell mediums were changed every 2-3 days and passaged when they reach 70-80 % confluency.

Table 3

List of cell lines and their growth mediums.

Cell Line	Type	Growth Medium
HT-29	Human Colorectal adenocarcinoma	10 % Fetal Bovine Serum, 100 µg/mL streptomycin, 100U/mL penicilin, DMEM
MCF-7	Human Breast adenocarcinoma	
HUVEC	Human umbilical vein endothelial	
PC-3	Human Prostatic adenocarcinoma	20 % Fetal Bovine Serum, 100 µg/mL streptomycin, 100U/mL penicilin, DMEM

3.2. Methods

Once triarylbenzophenone derivatives were synthesized by Dr. Lukas Rycek and transferred to our lab, the anticancer properties of compounds were determined by cytotoxicity tests, and the mechanism of actions of the lead compound was determined by cellular proliferation, cell migration, qPCR, and flow cytometry analyses. Furthermore, enzyme-based analyses and in silico molecular docking and molecular dynamics simulations were used to clarify the effect of the compounds on TOPO I and II dual inhibition.

3.2.1. Cell Cytotoxicity Analyses

Sulforhodamine B (SRB) assay was performed to determine the antiproliferative effect of triarylbenzophenone derivatives on MCF-7, HT-29, PC-3, and HUVEC cells. Cells

were plated on 96-well plates with 50000 cells/well concentration. After cell attachment, cells were treated with different doses of compounds for 48 hours. After incubation, cells were fixated with trichloroacetic acid (TCA) (10% (m/V)) solution for an hour at 4 °C. Then, the excess amount of TCA was removed by dH_2O washing and air-dried. After that, 100 µL of SRB dye (0.04% m/V) was added to cells and incubated for half an hour at RT. After incubation, the unbound SRB dye was discarded and the cells were washed with 1% (V/V) acetic acid solution. Finally, Tris base solution (10 mM, pH: 10.5) was added to each well and absorbance was measured spectrophotometrically at 565 nm. IC_{50} values of the compounds were determined by GraphPad Prism 8 software.

3.2.2. Cell Migration Assay

The effect of the lead compound on the migration ability of whole-cell masses was elucidated by wound healing assay. For analysis, PC-3 and HT-29 cells were seeded on a 24-well plate at $7x10^5$ cells/well density and incubated for 24 h. The artificial linear wound was generated by using 200 µL sterile pipette tips and wells washed with PBS (1X). After supplying fresh media, cells were treated with IC_{50} and two-fold IC_{50} doses of the compound. The image of wounds was taken with an inverted microscope at 12h time intervals. The percentage of wound closure was measured by using Image J software.

3.2.3. Cell Proliferation Assay

Colony formation assay was performed to determine the proliferation capability of cancer cells in the presence and absence of lead compound. Briefly, PC-3 cells were seeded into 6-well plates with the concentration of 1000 cells/well density and incubated for 24 hours. Then, cells were treated with determined doses (IC_{50} and two-fold IC_{50}) of compounds for 48 hours. After 48 h incubation, the medium was aspirated from the wells and replaced by a fresh cell culture medium. The media in wells were changed every 2-3 days until enough cells for colony formation (approx. 50 cells) were observed in wells. Then, each well was washed with PBS (1X) and fixed with acetic acid + methanol solution (1:3) for 30 mins. After incubation time is finished, 1 mL of Crystal Violet (5 % m/V) was poured onto cells

and incubated for 30 min at RT. Then, The number of colonies was determined by ImageJ software.

3.2.4. Annexin V and PI Assays

The effect of compounds on apoptosis and cell cycle arrest was determined by flow cytometry analysis. Briefly, HT-29 and PC-3 cells were seeded on a 6-well cell culture plate with a concentration of 550000 cells/well. After cell attachment, cells were treated with determined doses of compound (IC50 and two-fold IC50) for 48 hours. After incubation, cells were collected with trypsin-EDTA. Then, samples were analyzed using a flow cytometer.

3.2.5. Determination of Autophagic Gene Expression

For evaluation of autophagic effect of lead compounds qPCR analyses were performed. After treatment with lead compounds RNA isolation and cDNA synthesis was carried out as previously described by Tumer et al. (2018). The expression levels of LC-3 and Beclin-1 and ß-actin genes were investigated using specific TaqMan ® probes. The relative change in gene expression was calculated by using the comparative ΔΔCt method.

3.2.6. Topoisomerase I and II DNA Relaxation Assays

The effect of lead compounds on TOPO I and II enzyme activity was determined by agarose gel electrophoreses-based enzyme inhibition assay. The assays-based relaxation of supercoiled DNA plasmid by topoisomerase enzymes. TOPOGEN topoisomerase I inhibition assay kit (TG1015-3A) was used as described in the manufacturer's specifications. Briefly, the TOPO I enzyme (2 U) was pre-incubated with or without compounds at 37°C for 30 mins in the reaction buffer supplemented in the kit. After incubation, the reaction volume was completed to 20 µl by the addition of 250 ng pHOT1 plasmid. The reaction

mixture was incubated at 37°C for 30 mins. Then, 4 µL stop solution was added to stop the reaction.

TOPOGEN topoisomerase II inhibition assay kit (TG1001-3A) was used for the determination effect of lead compounds on TOPO II enzyme activity with small modifications. Briefly, 250 ng pHOT1 plasmid and TOPO II enzyme (10 U) were incubated with or without compounds at 37°C for 30 mins in the reaction buffer supplemented in the kit. The reaction was terminated by the addition of a stop solution (5 µL). Groups in these assays showed below (Table 4).

Table 4

Groups in topoisomerase I and II DNA relaxation assays

Control (C)	Enzyme (E)	Test Compounds
1. 250 ng pHOT plasmid + reaction mixture	1. 250 ng pHOT plasmid 2. Reaction mixture 3. Topoisomerase I or II enzyme	1. 250 ng pHOT plasmid 2. Reaction mixture 3. Topoisomerase I or II enzyme 4. Test compound

DNA samples were electrophoresed on a 1% agarose gel at 100 V for 1 h with a running buffer of TAE (Tris-Acetate-EDTA). The gel was stained for 1 µg/ml SYBR® Green containing TAE buffer for 30 mins. DNA bands were visualized under UV light and analyzed by Image Studio v.5.2. Steps of TOPO I and II enzyme assays were given in figure 6. The percentage of topoisomerase enzyme activity was calculated by drawing a standard curve, according to the DNA band intensities of control and enzyme groups where the DNA band intensity of the control group represents the minimum and the DNA band intensity of the enzyme group represents the maximum enzyme activity.

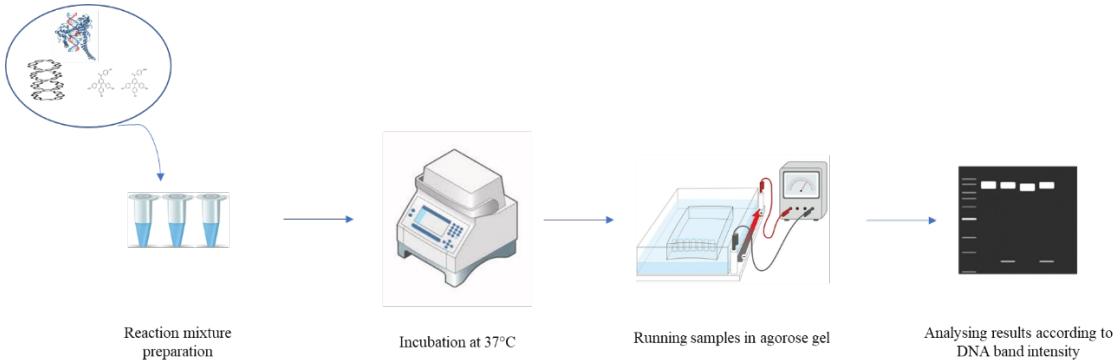

Figure 6. Steps for topoisomerase I and II DNA relaxation assays.

3.2.7. In silico Analyses

Interactions between triarylbenzophenone derivatives and topoisomerases were clarified utilizing combined molecular docking and molecular dynamics simulations.

Protein and ligand preparation

The 3D structures of TOPO I (PDB ID: 1sc7) and TOPO II (PDB ID: 4j3n) proteins, resolved by X-ray crystallography, were downloaded from the protein data bank (Berman et al., 2000). The resolutions of TOPO I and TOPO II were 3.00 Å and 2.30 Å, respectively. The crystal structure of TOPO I included Indenoisoquinoline, MJ-II-38 ligand molecules and 22 bp DNA duplex. Indenoisoquinoline and MJ-II-38 were removed from the structure, and mutations found in the position of Tdg 11 and Ptr 723 were swapped with Dg11 and Tyr 723 by using YASARA Structure (Krieger & Vriend, 2002) prior to molecular dynamics (MD) simulations. Structure of TOPO II included of 20 bp DNA Duplex. Missing amino acid residues between Thr 591-Ala 640, Leu 696-Lys 707, and Glu 1111-Gly 1135 in chain A and Pro 592-Ala 637, Gly 695-Thr 706, Asn 961-Pro967, and Gln1110-Gly1135 in chain B were completed using “build loop” tool in YASARA Structure. Missing amino acid sequence is provided as an input and this tool completes this sequence by comparing the same amino acid sequence with those in the protein data bank and assigns 3-D model. The protonation states of titratable amino acid side chains were determined by the PROPKA

server (Jurrus et al., 2018). This server predicts the protonation states by calculating pKa values according to the local environment of each and every amino acid side chain. Briefly, the server adds missing atoms according to the standard amino acid topologies. Then, the protein was treated by a force field, in this case, PARSE (Tang et al., 2007). pK_a of amino acids calculated by desolvation, hydrogen bonding, and charge–charge interactions.

Ligand molecules were sketched in ChemDraw Professional 16.0 (RRID: SCR 016768) and they were energy minimized in YASARA Structure software with NOVA2 force field. The protonation states of the ligands were computed according to the structures provided by Dr. Lucas Rycek. Energy minimized 3-D structures of reference molecules (Topotecan and Etoposide) compounds were obtained from the UCSF Chimera (Pettersen et al., 2004). PubChem database (Kim et al., 2023) identification numbers were provided as inputs; (PubChem CID: 60700 for topotecan and PubChem CID: 36462 for etoposide).

Molecular Dynamics (MD) Simulations

MD simulations were performed by GROMACS 5.1.4 program (Lindahl et al., 2001) employing AMBER03 force field (Ponder & Case, 2003) on the TUBITAK Ulakbim TRUBA server. Aforementioned processed structures of TOPO I and TOPO II were placed in cubic boxes with dimensions of 15 x 15 x 15 Å and 17 x 17 x 17 Å, respectively. Then, boxes were filled with SPC water molecules (Berendsen et al., 1987) and Na+ and Cl- ions for charge neutralization. After that, energy minimization was performed on the systems for 50,000 steps using the steepest descent method, with an energy minimization tolerance of 239 (kcal/mol)/nm and a step size of 0.01 nm. After energy minimization, 100 pico-second (ps) particle (N), volume (V), temperature (T); NVT and particle (N), pressure (P), and temperature (T); NPT balancing simulations were performed for each system. The bond length and angles of the water molecules were constrained by using the SETTLE algorithm (Miyamoto & Kollman, 1992). The bond lengths of the amino acid residues were utilized by the LINCS algorithm (Hess et al., 1997). Long-range electrostatic interactions were calculated by Particle-mesh Ewald (PME) approach (Darden et al., 1993). Water molecules/ions were placed separately into a bath at 310 K with a coupling constant of 0.1

ps under a constant pressure of 1 bar. The leap-frog algorithm (Hockney et al., 1974) was used to integrate the equation of motion at 2 femtoseconds (fs) time increments. The production simulations were run until the Root-mean-square deviation (RMSD) values of the structures reach to equilibrium. Regarding this, production simulations were run for 40 ns and 30 ns for TOPO I and TOPO II, respectively. At the end of simulations, "cluster" tool implemented in GROMACS 5.1.4 was used to acquire the most representative structure from time frame at which proteins reached equilibrium with a cut-off value of 0.3 nm.

The best docking poses, based on the highest binding affinity, were selected and these complexes were subjected to 50 ns MD simulations under the same conditions as detailed above. After the simulations are finished, snapshots were taken for each 1 ns of the last 10 ns of the simulations (the total of 10 structures) and the binding free energy of protein-ligand complexes was determined using the PRODIGY-LIGAND online server (Vangone et al., 2019).

Molecular Docking Simulations

Molecular docking simulations were performed by AutoDock Vina 1.1.2 program (Trott & Olson, 2010) implemented in YASARA Structure. Briefly, the most representative protein structures obtained from the MD simulations were placed in a grid box with the dimensions 64 Å X 64 Å X 64 Å, and 71 Å X 71 Å X 71 Å for TOPO I and TOPO II, respectively. Spacing was arranged to 1.00 Å and exhaustiveness set to 20. 25 poses were obtained and then they were clustered according to their binding mode and binding affinities.

3.2.8. Statistical Analyses

Significant differences and statistical analyses were performed on GraphPad Prism 8 software. Data were obtained through biological and computer-based analyses. Results were represented as the standard error of mean ± (SEM). One-way analysis of variance (ANOVA) was used to make the comparison between control and treatment groups.

CHAPTER 4
RESULTS AND DISCUSSION

4.1. Result

In this study, novel triarylbenzophenone derivatives were investigated for their anticancer effect and dual TOPO I and II inhibitory potentials. Briefly, the compounds were screened on prostate, colon and breast cancer cell lines. Also, healthy endothelial cell lines to evaluate whether these compounds have cytotoxic effects on noncancerous cells. Then, the most effective compound was selected according to IC_{50} values. The action mechanism of the lead compound was determined by in vitro cell-based cell proliferation, cell migration assays, flow cytometry and qPCR analyses. Additionally, TOPO I and II enzyme inhibition experiments were also carried out to assess the compounds' inhibitory effects on TOPO I and II. In silico molecular docking and molecular dynamics simulations were used to investigate the interactions between triarylbenzophenone derivatives and topoisomerase.

4.1.1. Evaluation of Cytotoxic Effect of Triarylbenzophenone Derivatives

The effect of triarylbenzophenone derivatives on cancer cell lines alongside with healthy cell lines were examined by SRB assay. Firstly, cells were treated with the highest dose of compounds (100 μM) for 48 h. According to the results, all the compounds decreased the cell viability of HT-29 and PC-3 cell lines lower than 50 %, except **SMR32-2**. Also, the compounds did not cause any cytotoxicity on the MCF-7 cell line. **SMR-36** inhibited the proliferation of HT-29, PC-3 and HUVEC cells by 78 %, 95 %, and 57 % respectively. **SBB** inhibited the proliferation of the cell lines by 71 %, 80 %, and 28 %, respectively (Figure 7).

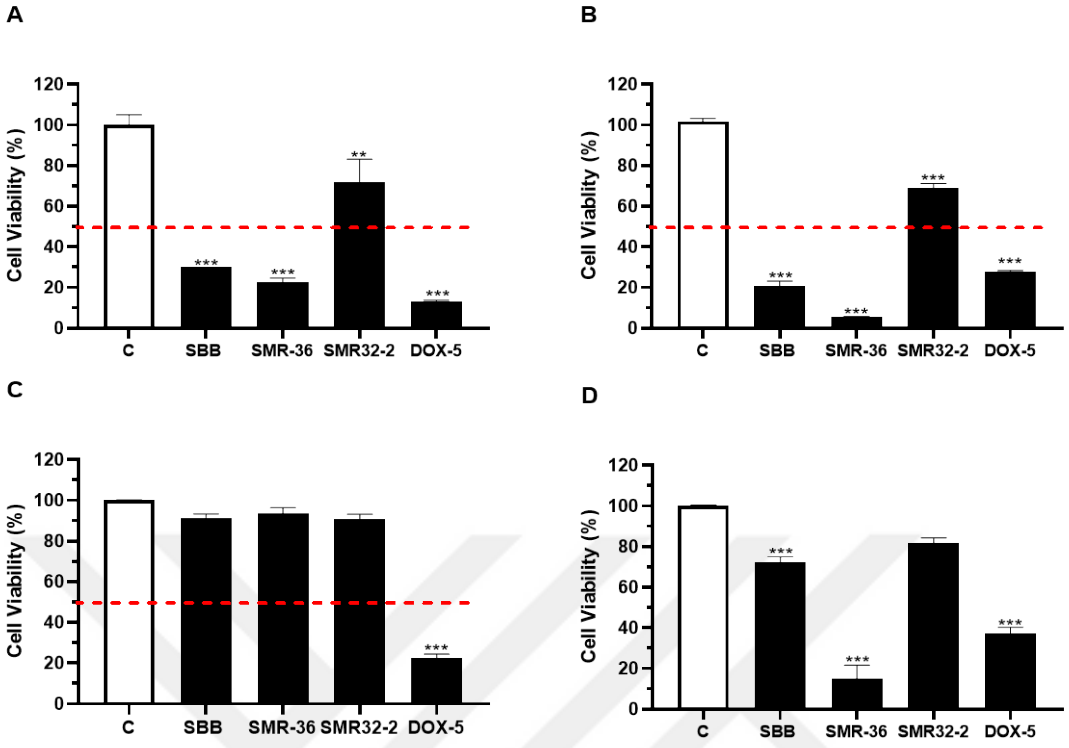

Figure 7. Effect of triarylbenzophenone derivatives on HT-29 (A), PC-3 (B), MCF-7 (C) and HUVEC (D) cell lines. C: Control. Dox-5: Doxurubicin 5 µM. **p < 0.005, ***p < 0.001.

After the screening of the triarylbenzophenone derivatives, **SMR-36** and **SBB** were selected due to their cytotoxic effect. After that, cells were treated with 1, 5, 10, 25, 50 and 100 µM doses of the selected compounds to calculate their IC_{50} values on cancerous and noncancerous cell lines. As shown in Table 5, IC_{50} values of **SMR36** in the HT-29, PC-3, MCF-7, and HUVEC cells were found as 17.6, 129.7, 5.9, and 73.8 µM, respectively. SI values for each compound have been determined by dividing the IC_{50} values of the healthy cell lines to the IC_{50} value of the cancerous cell lines. Accordingly, the SI of **SMR-36** on the cancer cell lines were calculated as 4.2, 12.3, and 0.5, respectively. IC_{50} values of **SBB** on the cells were calculated as 53.4, 1250, 79.9, and 1012 µM, respectively. SI of **SBB** on the cancer cell lines were determined as 18.9, 12.6, and 0.8, respectively. (Table 5). Accordingly, **SMR-36** was selected as a lead compound due to its low IC_{50} and SI on prostate and colon cancer cell lines.

Table 5

IC_{50} values and Selectivity index (SI) of **SMR-36** and **SBB**.

COMPOUND	IC_{50} ± SE (μM)				Selectivity Index (SI)		
	HT-29	MCF-7	PC-3	HUVEC	HT-29	MCF-7	PC-3
SMR-36	17.6 ± 3.0	129.7 ± 40.8	5.9 ± 1.0	73.8 ± 18.6	4.19	0.5	12.3
SBB	53.4 ± 29.5	1250 ± 392.5	79.9 ± 28.9	1012 ± 471.3	18.96	0.8	12.6

4.1.2. Effect of SMR-36 on Cell Migration and Cell Proliferation

The effect of **SMR-36** on cell proliferation and migration of HT-29 and PC-3 cells were examined by colony formation and wound healing assays. Cells were treated with IC_{50} and two times IC_{50} doses of **SMR-36** for 48 hours. Accordingly, **SMR-36** application significantly reduced the wound recovery of PC-3 cells in a dose dependent manner (58 % and 59 %, respectively) (Figure 8).

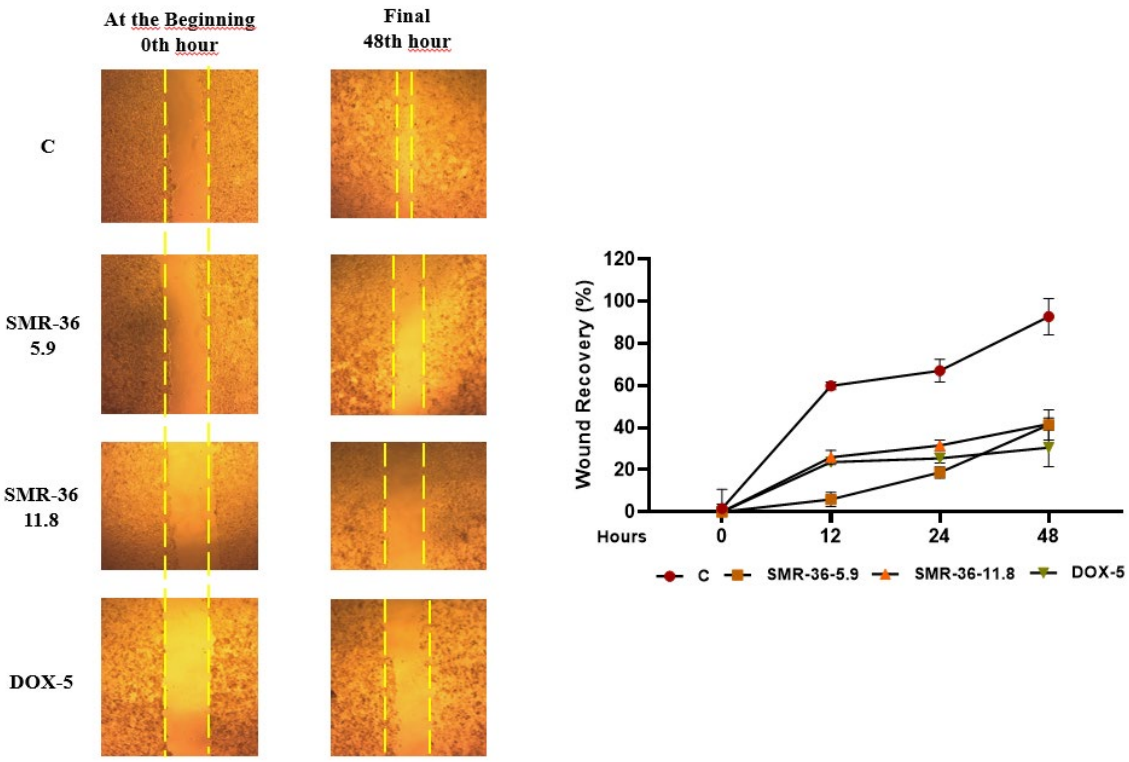

Figure 8. Effect of **SMR-36** on wound recovery capability of prostate cancer cells. C: Control. Dox-5: Doxurubicin 5 µM.

IC_{50} and two times IC_{50} doses of **SMR-36** were significantly reduced the wound recovery of HT-29 cells by 10 % and 56 %, respectively. Reference compound doxorubicin inhibited the wound recovery of the cells by 39 % (Figure 9).

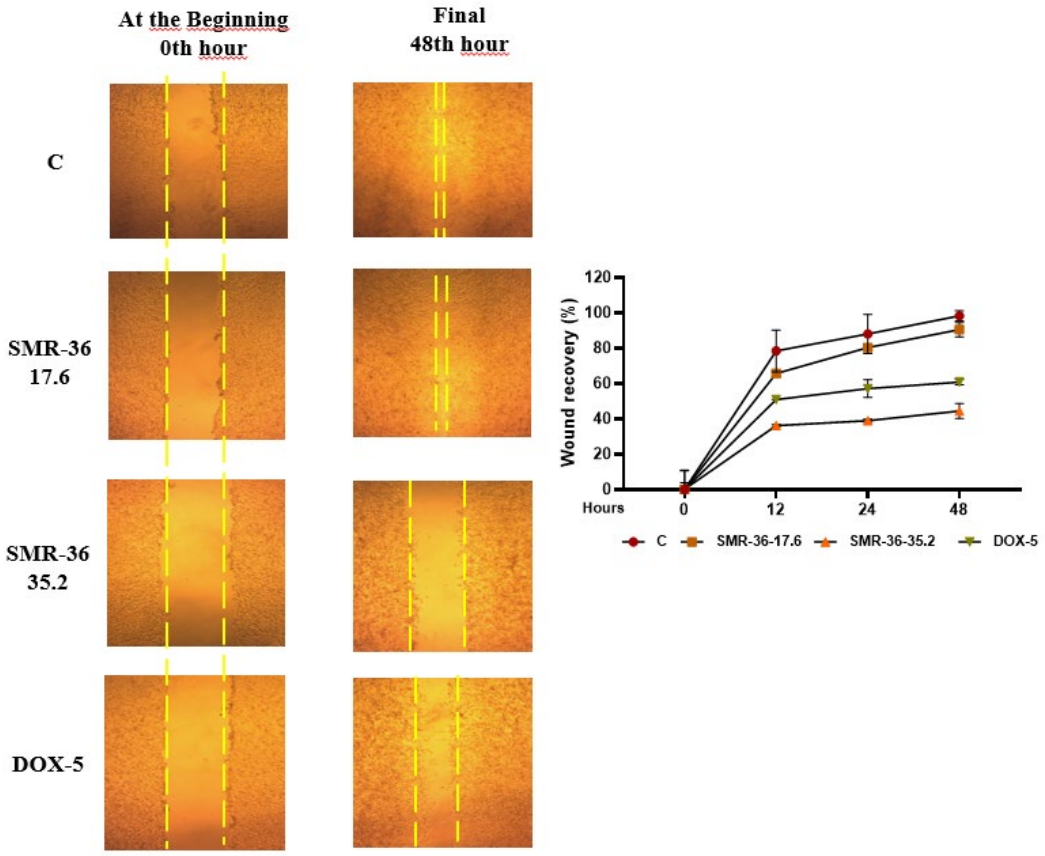

Figure 9. Effect of **SMR-36** on wound recovery capability of colon cancer cells. C: Control. Dox-5: Doxurubicin 5 µM.

The effect of **SMR-36** on cell proliferation was evaluated by colony formation assay. Regarding this, cells were treated with IC_{50} and two times IC_{50} doses **SMR-36** and cells were observed until enough colonies are formed (approximately 50 cells in one colony). As shown in Figure 11, **SMR-36** application significantly inhibited colony formation of PC-3 cells in a dose-dependent manner (53 % and 87 % respectively). Also, two doses of **SMR-36** application was decreased the colony formation of HT-29 cells by 44 % and 92 % (Figure 10).

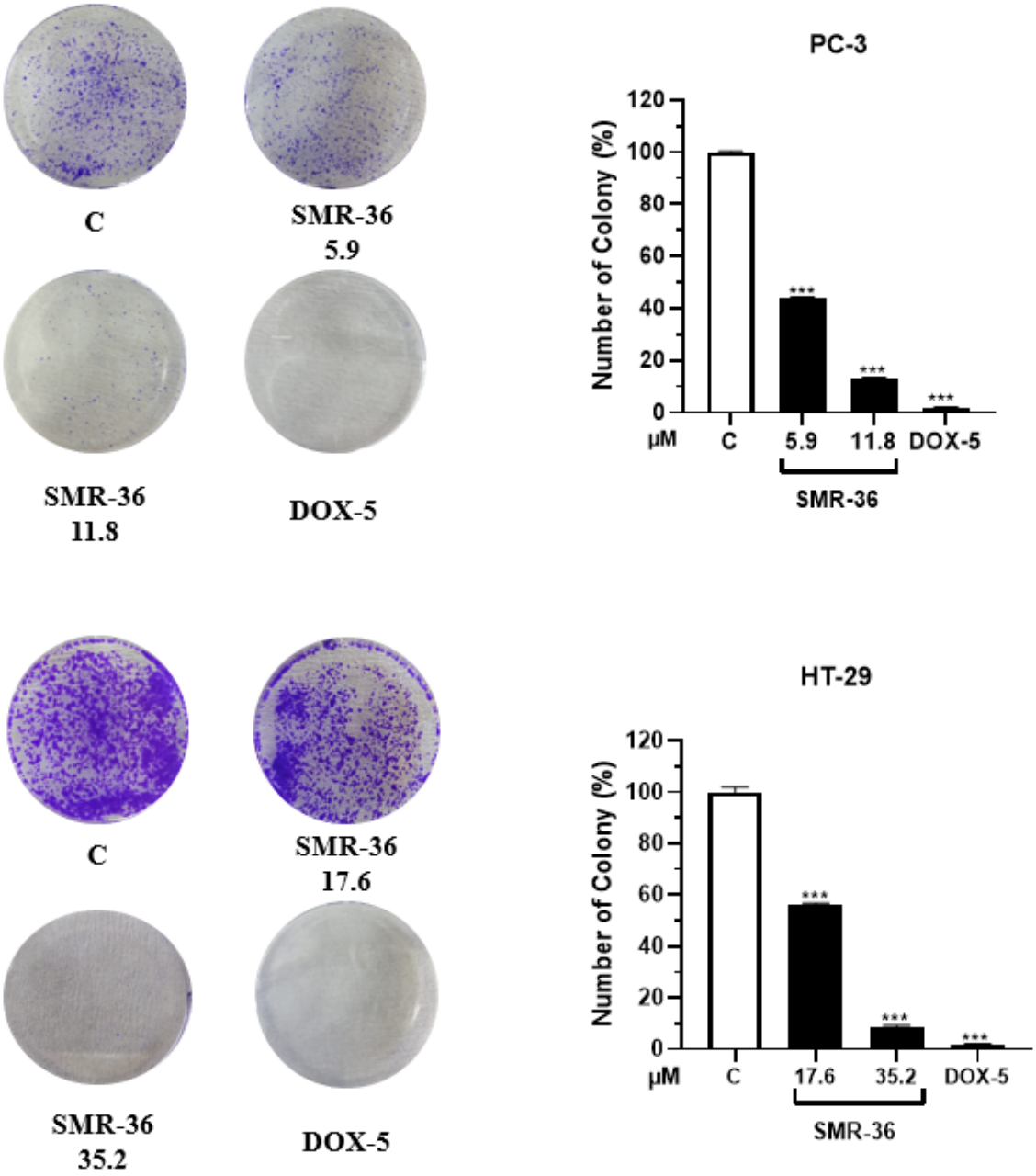

Figure 10. Effect of **SMR-36** on colony formation of PC-3 (up) and HT-29 (down) cells. C: Control. Dox-5: Doxurubicin 5 µM. ***p < 0.001.

4.1.3. Effect of SMR36 on Apoptosis and Cell Cycle Arrest

Flow cytometry analyses were conducted to examine the impact of SMR-36 on the percentage of apoptotic cells and cell cycle arrest. These analyses were carried out at the

laboratory of Prof. Dr. Feray Köçkar at Balıkesir University. Following the cell treatment, the cells were collected in the treatment medium and subsequently transferred to Balıkesir for further analysis. The results indicate that the application of SMR-36 did not induce apoptosis in either PC-3 or HT-29 cells. (Figure 11).

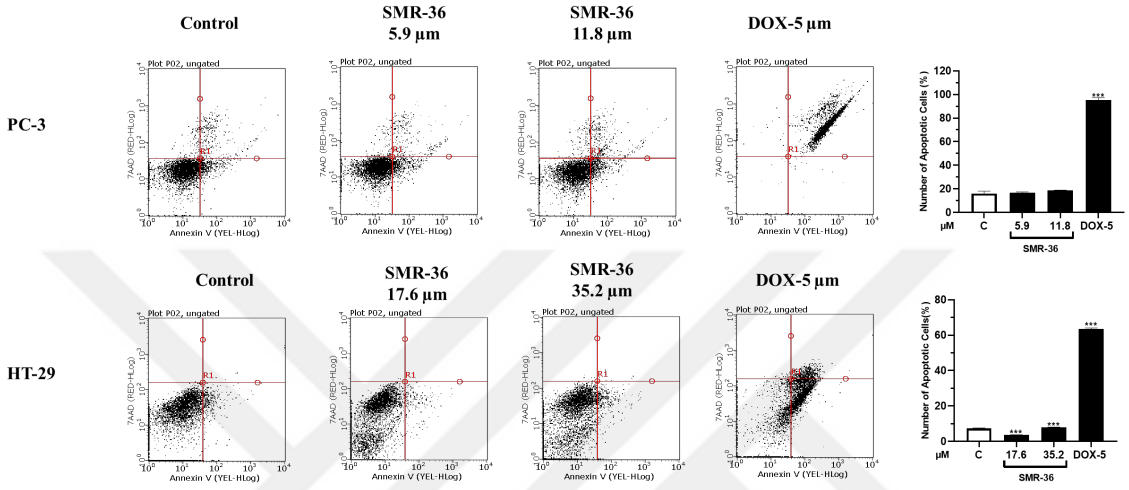

Figure 11. Effect of **SMR-36** on apoptotic cell percentage of PC-3 and HT-29 cells. The bottom left quarter indicates alive cells; the bottom right quarter indicates early apoptotic cells; the upper right quarter indicates late apoptotic cells; the upper left quarter indicates necrotic cells. C: Control. Dox-5: Doxurubicin 5 µM. ***$p < 0.001$.

Additionally, both **SMR-36** and doxorubicin application did not induce cell cycle arrest at PC-3 and HT-29 cells (Figure 12).

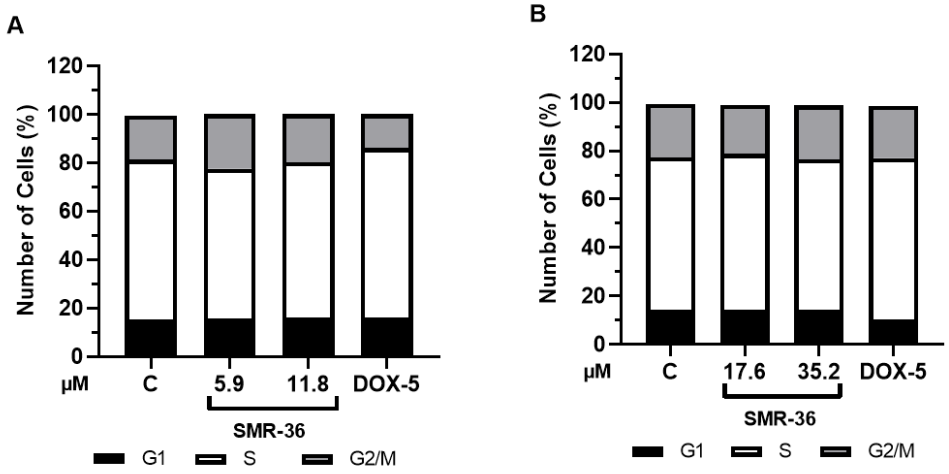

Figure 12. Effect of **SMR-36** on cell cycle arrest on PC-3 (A) and HT-29 (B) cells.

4.1.4. Effect of SMR36 on Autophagic Gene Expression

The effect of **SMR-36** on autophagic gene (LC-3 and Beclin-1) expression levels were determined on PC-3 cells. Regarding this, the cells were treated with **SMR-36** for 48 h**.** Then, RNA isolation and cDNA synthesis were completed, respectively. The expression level of the aforementioned genes were examined by qPCR analyses. As shown in Figure 14, the **SMR-36** application did not induce autophagic gene expressions (Figure 13).

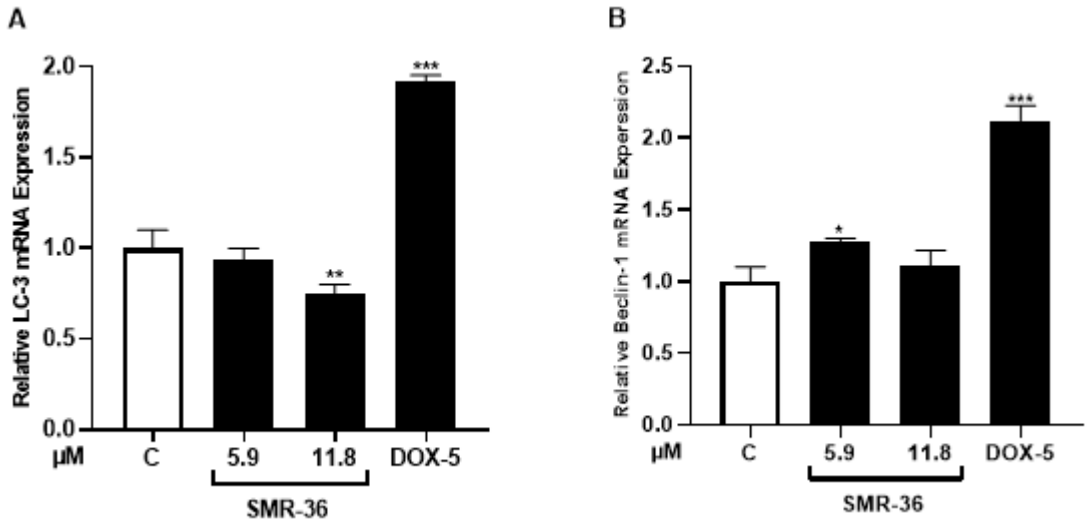

Figure 13. Effects of **SMR-36** on LC-3 (A), and Beclin-1 (B) mRNA expression levels in PC-3 prostate cancer cells. *p< 0.02, **p< 0.005, ***p < 0.001.

4.1.5. Effect of SMR36 and SBB on Topoisomerase activity

The effect of the **SMR-36** and **SBB** on topoisomerase enzymes were screened by using TOPOGEN topoisomerase I and II enzyme assay kits. Firstly, a screening was performed using a concentration of 1 µM for the compounds to evaluate their inhibitory impact on both TOPO I and TOPO II. As a result, it was observed that all the compounds exhibited a significant inhibition of TOPO I enzyme activity, surpassing a 50% inhibition. Among them, 1 µM of **SMR-36** and **SBB** were inhibited enzyme activity approximately 51 and 76 %, respectively. Also, **SMR-36** was inhibited TOPO II enzyme activity 89%, while, **SBB** application inhibited enzyme activity only 30% (Figure 14).

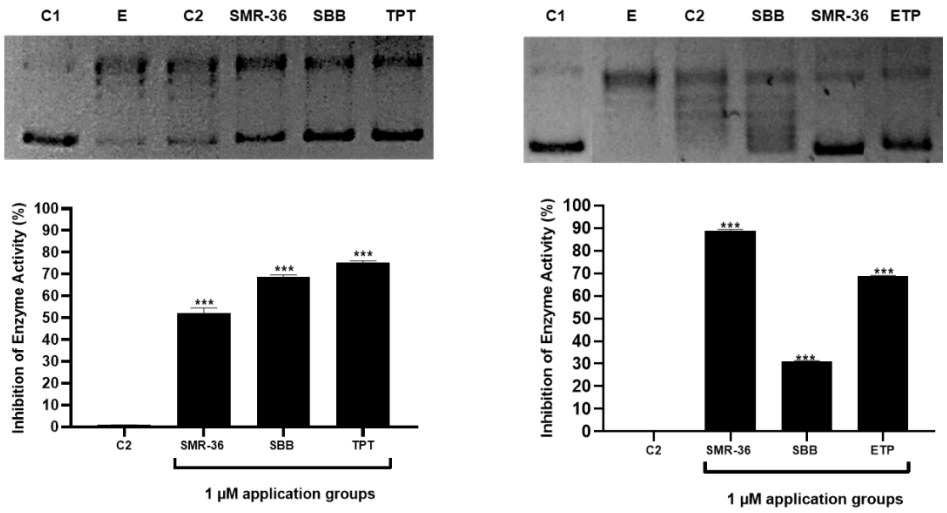

Figure 14. Triarylbenzophenone derivatives inhibited dual topoisomerase I (A) and II (B). Lane C1: Control 1 (pHOT1 plasmid (250 ng)). Lane E: Enzyme (pHOT1 plasmid (250 ng) + Topoisomerase enzyme (2U for Topoisomerase I (left), 10U for Topoisomerase II (right)). Lane C2: Control 2 (pHOT1 plasmid (250 ng) + Topoisomerase enzyme (2U for Topoisomerase I (left), 10U for Topoisomerase II (right)) + DMSO (1%). Other Lanes: pHOT1 plasmid (250 ng) + Topoisomerase enzyme (2U for Topoisomerase I (left), 10U for Topoisomerase II (right)) + 1 µM of the compounds.***$p < 0.001$.

4.1.6. In silico assessment of interactions between triarylbenzophenone derivatives and Topoisomerases

Preparation of TOPO I/II Interactions between triarylbenzophenone derivatives and topoisomerases were evaluated by in silico molecular docking and molecular dynamics simulations. Firstly, 3D structures of TOPO I/II and triarylbenzophenone derivatives were prepared for computational based analyses as described in section 3.2.7. Then, MD simulations were performed by GROMACS 5.1.4 program until the RMSD value of each structure reach to equilibrium. Regarding this, TOPO I and TOPO II were subjected to 40 and 30 ns production simulations, respectively (Figure 15). The most representative structure was taken from the last 10 ns of the simulations.

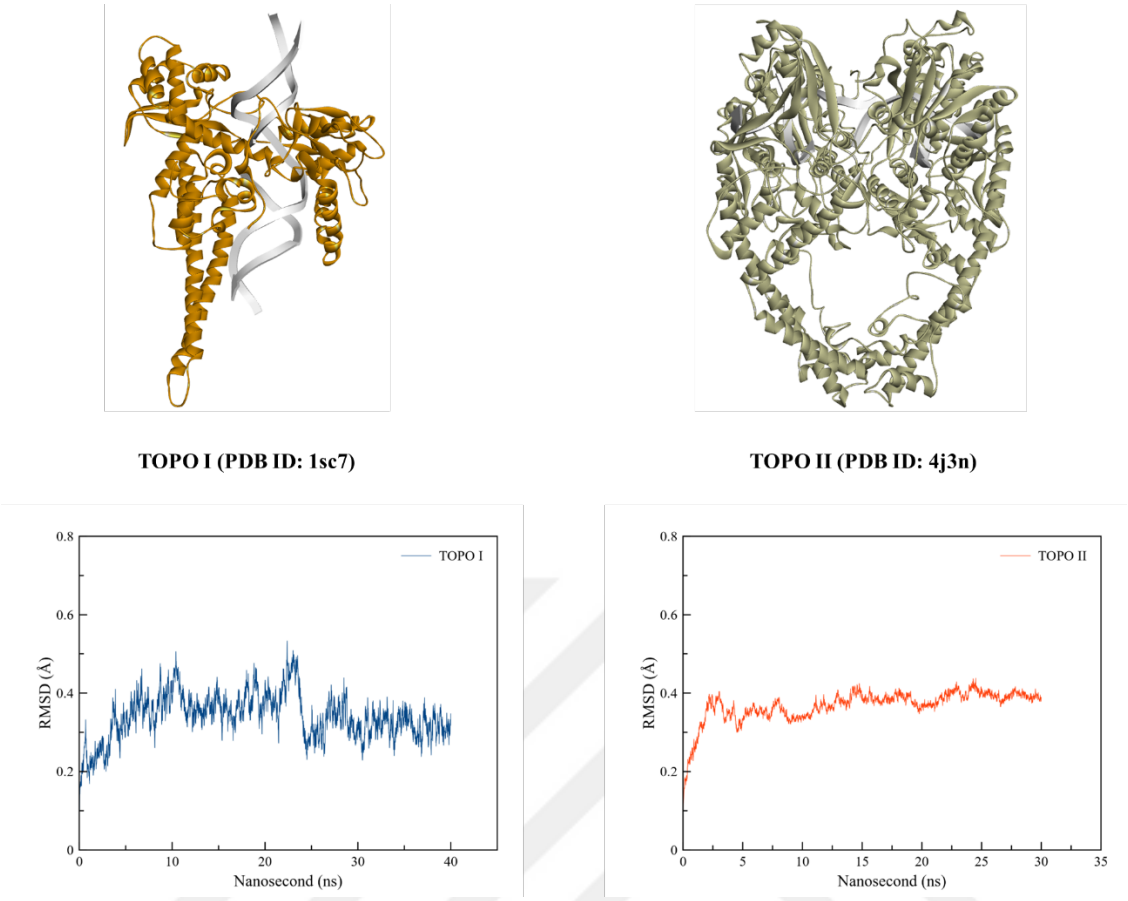

Figure 15. 3D structure of TOPO I and II (up) and RMSD values of TOPO I and II at the end of the MD simulations.

Binding affinity of triarylbenzophenone derivatives to TOPO I and II

Molecular docking analyses were conducted using YASARA Structure, which utilizes AutoDock Vina for molecular docking simulations. The results of the analysis revealed that **SBB** and **SMR-36** bounded to TOPO I, exhibiting binding affinities of -10.2 (the first pose of SBB) /-10.1 (the second pose of SBB) and -9.9 kcal/mol, respectively. In comparison, the reference molecule topotecan bound to the active site of TOPO I with a binding affinity of -8.9 kcal/mol. Furthermore, the compounds displayed similar binding affinities towards TOPO II (-9.1 and -9.2 kcal/mol), while the reference molecule etoposide (ETP) bound to TOPO II with a binding affinity of -10.2 kcal/mol. (Table 6).

Table 6

Binding affinities of triarylbenzophenone derivatives to topoisomerase I and II. Standart Error (SE) was calculated using the binding free energy difference between poses taken from the last 10 ns of the simulation.

Compound	Topoisomerase I	Topoisomerase II
	Binding Affinity (kcal/mol)	
SBB	-10.2/-10.1	-9.1
SMR-36	-9.9	-9.2
TPT	- 8.9	
ETP		-10.2

Binding stability of triarylbenzophenone derivatives in the TOPO I and II

Following the molecular docking simulations, MD (molecular dynamics) simulations were carried out to assess the binding stability of the compounds with the topoisomerases. For this analysis, the best docking poses of the compounds were subjected to MD simulations until RMSD values of the systems reached to equilibrium. For TOPO I, the two best poses of **SBB** were selected due to a small binding affinity discrepancy between the poses (0.01 kcal/mol). At the end of the simulations, the binding free energy of the taken snapshots were determined using the PRODGY-LIGAND online server (Vangone et al., 2019). According to the results, the RMSD values of the systems were equilibrated at the end of 50 ns simulations (Appendix-Figure 1). Also, both **SMR-36** and **SBB** remained in the binding sites of topoisomerases (Figure 16).

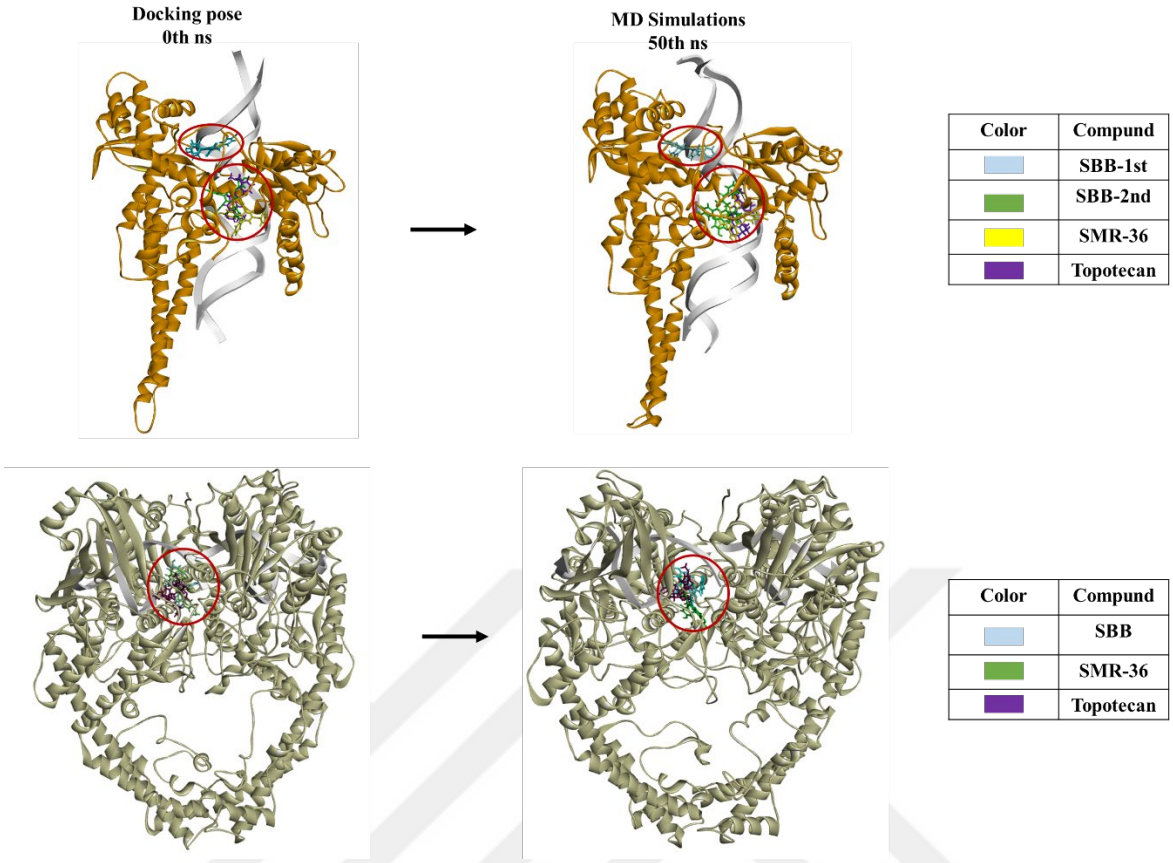

Figure 16. Positions of the **SBB**, **SMR-36**, and reference molecules at molecular docking (left) and the end of 50 ns MD simulations (right).

SMR-36 remained bound to the binding site of both TOPO I and TOPO II, exhibiting binding energies of -13.6 and -13.2 kcal/mol, respectively. On the other hand, **SBB** interacted with TOPO I and TOPO II, with binding energies of -10.8/-13.6 and -14.3 kcal/mol, respectively. (Table 7).

Table 7

Binding free energies of triarylbenzophenone derivatives to topoisomerase I and II. SE

Compound	Topoisomerase I	Topoisomerase II
	Binding Energy ± SE (kcal/mol)	
SBB	-10.8 ± 0.2 / -13.6 ± 0.3	-14.3 ± 0.2
SMR-36	-13.6 ± 0.2	-13.2 ± 0.2
TPT	-8.9 ± 0.2	
ETP		-12.7 ± 0.5

Interactions between SBB, SMR-36 and TOPO I

Interactions between the compounds and topoisomerases after molecular docking and MD simulations were visualized by Discovery Studio 2021 Client software (BIOVIA, Dassault Systeèmes, Discovery Studio Client, San Diego: Dassault Systeèmes, 2021). Accordingly, triarylbenzophenoen derivatives were stayed in their binding site to topoisomerases. **SMR-36** and the second best pose of **SBB** were protected their interactions with Arg 349, Ala 351, Lys 354, and Pro 431 residues of TOPO I at the end of MD simulations. On the other hand, the best docking pose of **SBB** yielded interactions with Dc 8, Lys 216, Lys 439, and Arg 449 residues of TOPO I in both docking and MD simulations. Reference molecule topotecan was protected its interactions with Dg 11, Dg 12, Dt 109, Dc 111, and Ala 351 residues of TOPO I (Figure 17).

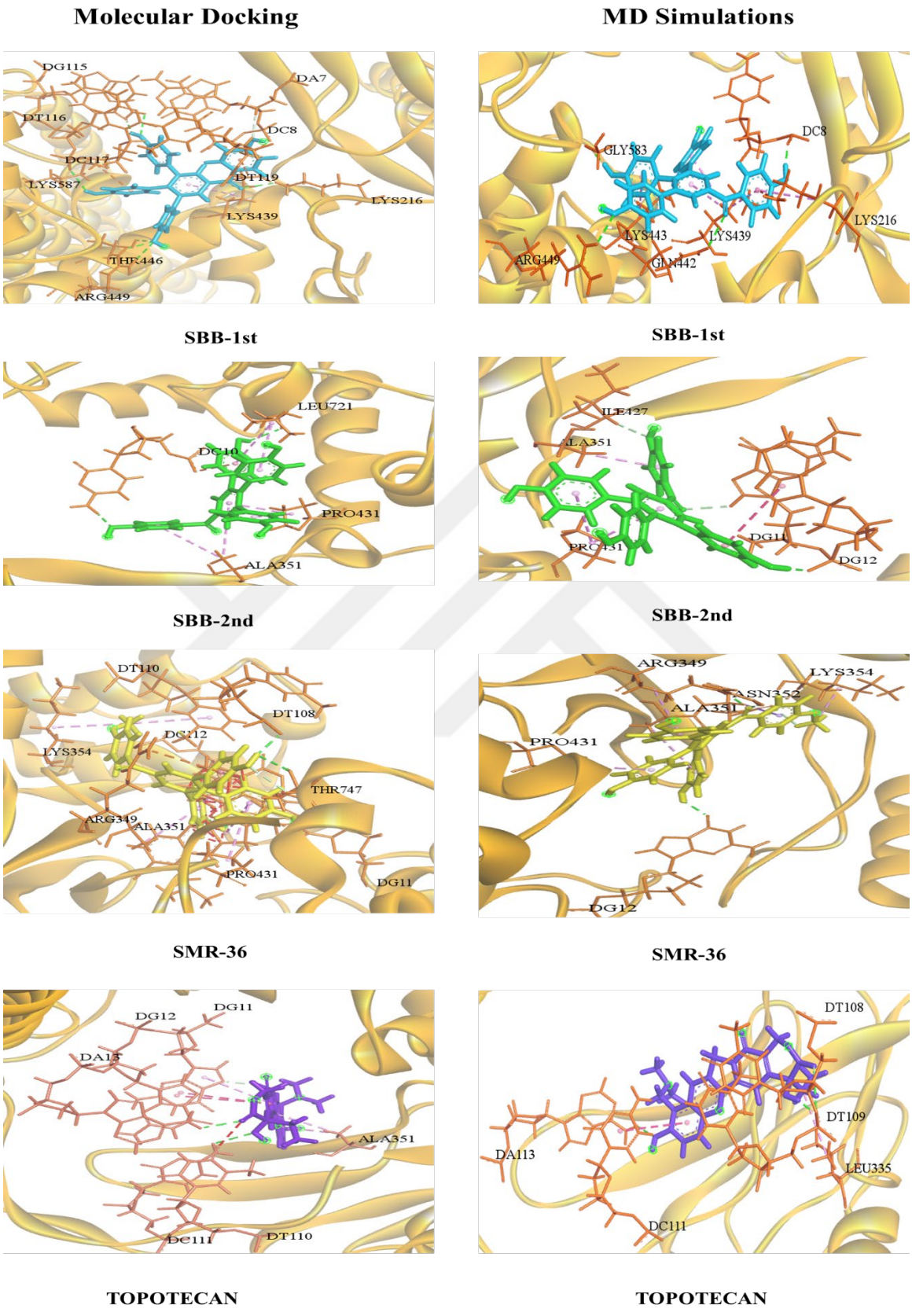

Figure 17. 2D representation of interactions between triarylbenzophenone derivatives and TOPO I at molecular docking and the end of 50 ns MD simulations. The first pose of **SBB**

showed as cyan, the second of **SBB** showed as green, **SMR-36** showed as yellow, topotecan showed as purple. Green lines represent hydrogen bonding interactions, pink lines represent π-π interactions, purple lines represent π-alkyl interactions, and orange lines represent π-sulfur interactions.

Interactions between SBB, SMR-36 and TOPO II

According to Figure 18, **SBB** protected its interactions with Da 12, Glu 777, and Arg 820, residues of TOPO II at the end of MD simulations. **SMR-36** yielded interactions with Dt 9, Gln 778, and Arg 820 residues of TOPO II in both docking and MD simulations. Reference molecule etoposide retained its interactions with Dg 7, Dc 8, Dc 11, and Ala 779 residues of TOPO II (Figure 18).

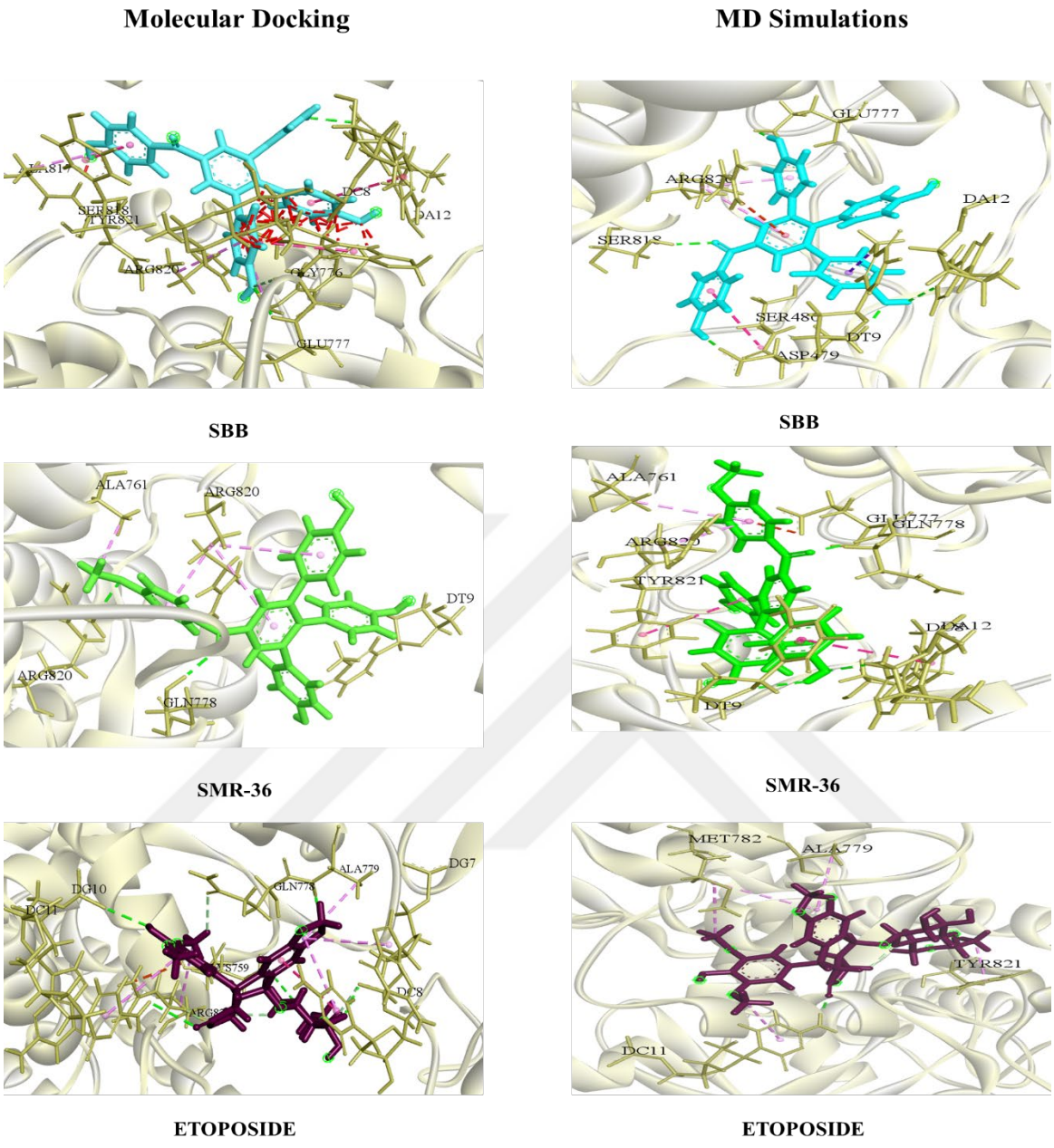

Figure 18. 2D representation of interactions between triarylbenzophenone derivatives and TOPO II. **SBB** showed as cyan, **SMR-36** showed as green, etoposide showed as purple. Green lines represent hydrogen bonding interactions, pink lines represent π-π interactions, purple lines represent π-alkyl interactions, and orange lines represent π-sulfur interactions.

4.2 Discussion

Natural-based compounds are still the main source of marketed anticancer drugs. According to recent records, 247 drugs have been approved for cancer treatment by world authorities (FDA, EMA, etc.) and approximately 50% of approved anticancer drugs are natural product derivatives or biosimilars (Choudhari et al., 2020). *Selaginella* plants have been used for the treatment of some anti-inflammatory diseases in China. Recently, it is implicated that compounds synthesized from *Selaginella* plant species were effective to inhibit cancer cell proliferation without leading to any cytotoxic effect on the healthy cell lines. Additionally, the compounds inhibited prostate cancer cell proliferation due to their inhibitory effect on PDE4D2 enzyme which is a biomarker for prostate cancer. Correlatively, in this study, triarylbenzophenone derivatives were selectively inhibited cell proliferation of the prostate cancer cell line (PC-3). The IC_{50} value of the **SMR-36** was found lower than 10 μM on the PC-3 cell line. Also, **SMR-36** showed moderate cytotoxicity on the HT-29 cell line (IC_{50} value of 17.6 μM). On the other hand, **SBB** had the highest SI index for both prostate and colon cancer cells (18.9 and 12.6, respectively). However, the IC_{50} values of the compound on the cells were higher than **SMR-36**. The main difference between the structure of triarylbenzophenone derivatives was their number of hydroxyl (-OH) and methoxy (-OMe) groups. In most cases, the addition of the methoxy groups to the structure of the compounds were increasing the cytotoxic effect (Liew et al., 2020). Correlatively, **SMR-36** showed a higher cytotoxic effect than **SBB**, while **SMR32-2** showed the lowest cytotoxic effect even though the compound has the highest number of methoxy groups compared to others. This may be explained by possible decrease in the cytotoxic potential of compounds after the replacement of the hydroxyl group with the methoxyl group (Lapinskaite et al., 2023).

SMR-36 were selected as a lead compound due to its promising potency and high selectivity against prostate and colon cancer cell lines. After that, the anticancer action mechanism of the compound was determined by wound healing and colony formation analyses. According to the results, **SMR-36** application decreased both colony formation and wound recovery of colon and prostate cancer cell lines. These results suggest that the invasiveness of prostate and colon cancer cells might be inhibited by **SMR-36** application.

Apoptosis and autophagy are two types of programmed cell deaths regulating cellular and organismal homeostasis. LC-3 and Beclin-1 are two regulatory proteins of autophagy. Increase in the expression level of the proteins associated with autophagosome formation. In this study, the effects of the **SMR-36** application on the expression level of the aforementioned genes were examined by qPCR analyses. Accordingly, the **SMR-36** application was induced any autophagic gene expression level. Additionally, apoptotic cell percentage after **SMR-36** treatment was determined by flow cytometry analyses and **SMR-36** application was not able to increase the number of apoptotic cells and cell cycle arrest. Overall, even though the compound has been found effective on cell proliferation and migration, **SMR-36** might not be able to induce apoptosis and autophagy on cancer cell lines and the possible effect of the compound on cell death need to be investigated.

Targeting multiple biological molecules with one compound is a recently used approach for cancer treatment, for example, dual topoisomerase I and II inhibition. Topoisomerase enzymes took a proactive role in both DNA replication and transcription processes and over-activation of the enzymes was associated with the cancer cell proliferation. Thus, there are multiple agents were developed to inhibit the activity of topoisomerases. The structure of the triarylbenzophenone derivatives was similar to the known topoisomerase inhibitors. Regarding this, the effect of the compounds on the topoisomerase enzymes was determined by agarose-gel electrophoreses-based enzyme inhibition assay. According to the results, 1 μM dose **SMR-36** inhibited both TOPO I and TOPO II enzyme activity by 51 and 88 %, respectively. On the other hand, the same dose of **SBB** only inhibited the activity of TOPO I higher than 50 % (68 %). In summary, **SMR-36** appears to have the potential to act as a dual inhibitor of both TOPO I and II, whereas **SBB** might be a selective TOPO I inhibitor.

Molecular docking simulations is one of the most frequently used approach, uses in a variety of fields such as drug discovery, structure-activity studies, and virtual screening studies, for understanding and predicting of binding modes of two molecules. Prediction of the best binding mode is determined based on binding affinity. In the current study, firstly,

the binding mode of triarylbenzophenone derivatives to topoisomerases were evaluated by molecular docking simulations. The simulations were performed by the AutoDock Vina program implemented in YASARA Structure. According to the results, **SBB** and **SMR-36** bounded to the TOPO I and TOPO II with similar binding affinities. Surprisingly, **SBB** interacted with two different regions of the TOPO I with similar binding affinities (-10.2 and -10.1 kcal/mol). In the first pose, **SBB** performed hydrogen bonding and π-sulphide interactions with the DNA residues of TOPO I**,** while in the other pose, the compound mostly performed π- π interactions with the Ala 351, Pro 431 and Leu 721 residues of the DNA binding site of TOPO I. On the other hand, **SMR-36** interacted with Dg 11, Dt 108, Dc 112, Ala 351, Pro 431, and Tyr 747 residues of TOPO I through hydrogen bonding and π- π interactions. Also, **SMR-36** yielded 0.2 kcal/mol lower binding affinity to the TOPO I, the binding energy difference might be related to its low number of π- π interactions with TOPO I compared to **SBB**. For TOPO II, both compounds were interacted with the Dt 9, Glu 777, Arg 820, and Tyr 821 residues of TOPO II. Additionally, Both **SBB** and **SMR-36** have the same number of hydrogen bonding and π- π interactions with the aforementioned residues, while, **SMR-36** yielded a higher number of van der Waals interactions. The high number of van der Waals interactions between the compound and TOPO II might be an explanation for its stronger binding, in terms of binding affinity, to the TOPO II than **SBB** (Figure 19).

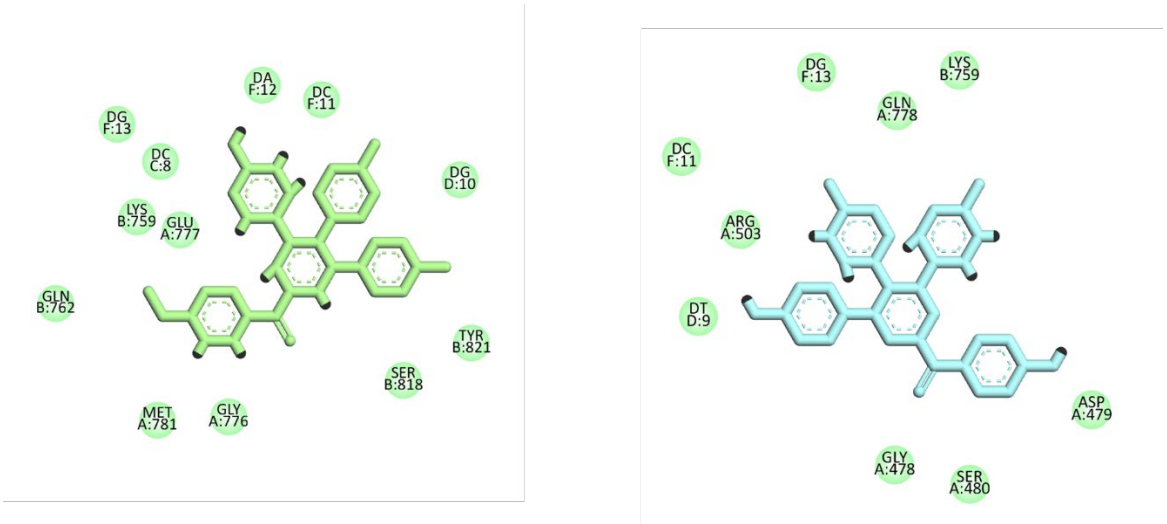

Figure 19. Van der Waals interactions between **SMR-36** (left), **SBB** (right) and TOPO II at the molecular docking simulations.

MD simulations is a computational method utilized to forecast the dynamic motion of atoms and molecules. It relies on Newton's law of motion (F=ma) as its underlying theory. In this equation, F represents the force exerted on a particle, m denotes its mass, and a signifies the resulting acceleration. By utilizing this equation, it becomes feasible to determine the changes in particle positions, velocities, and accelerations over time. Regarding this, the binding stability of triarylbenzophenone derivatives in the binding site of TOPO I and II were determined by MD simulations. Accordingly, triarylbenzophenone derivatives were stayed in their binding site with higher binding free energy than reference compounds. As shown in Figure 17, the first pose of **SBB** lost most of its docking interactions with DNA residues of TOPO I and performed interactions with the Lys 439, Arg 449, GLY 583, and Gln 442 residues of TOPO I, while the second pose of **SBB** protected its docking interactions. Also, both poses of **SBB** performed the similar number of hydrogen bonding and π- π interactions, However, there was a 2.8 kcal/mol binding free energy difference between the two poses of **SBB**. The reason behind the binding free energy discrepancy could be a higher number of van der Waals interactions between the second pose of **SBB** and TOPO I than the first pose of **SBB** (Figure 20). **SMR-36** was protected its docking interactions with Dt 108, Ala 351, Lys 354, and Pro 431 residues of TOPO II. Also, the compound and the second pose of **SBB** yielded the same binding free energy (-13.5 kcal/mol). For TOPO II, both compounds were interacted with similar residues in the active site of TOPO II. **SBB** performed higher number of hydrogen bonding interactions with TOPO II than **SMR-36**. The high number of hydrogen bonding interactions between **SBB** and TOPO II might be an explanation for its 1.1 kcal/mol stronger binding to TOPO II than **SMR-36**.

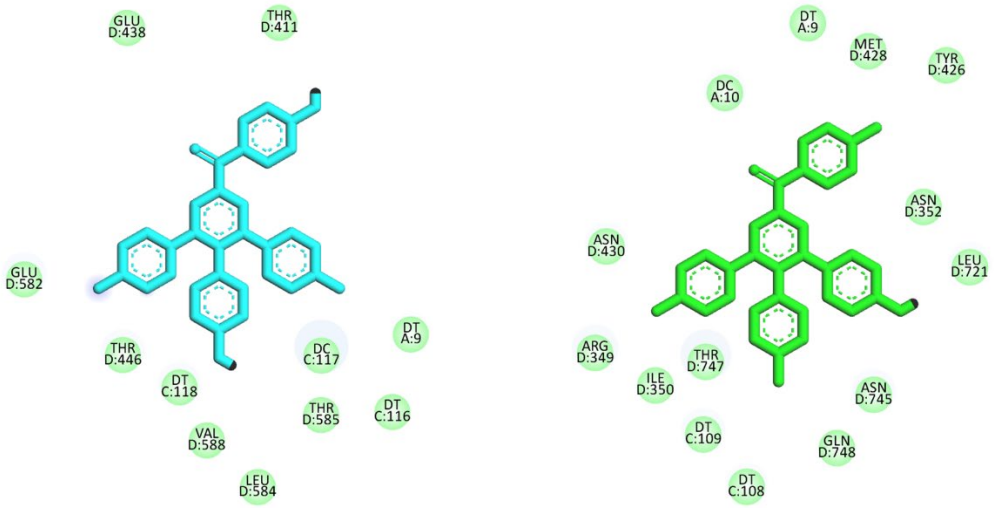

Figure 20. Van der Waals interactions between the first (left) and the second (right) pose of **SBB** and TOPO I at the end of 50 ns MD simulations.

CHAPTER 5
CONCLUSION

In this study, the anticancer effect and dual TOPO I and TOPO II inhibitory potential of three novel triarylbenzophenone derivatives were evaluated *in vitro* and *in silico* based analyses. Among the compounds, **SBB** and **SMR-36** showed selective antiproliferative activity against HT-29 colon cancer and PC-3 prostate cancer cell line. However, **SMR-36** was selected as a lead compound according to its low IC_{50} values (5.9 μM) on the prostate and colon cancer cell lines. Then, the compound was found effective on the migration capability of the cancer cell lines. However, the compounds are not able to induce expression level of apoptotic and autophagic genes, Regarding this, the effect of the compounds on cell death further need to be investigated. Furthermore, the effect of the compounds on TOPO I and TOPO II enzyme activity was measured. Dual inhibition of TOPO I and TOPO II overcomes drug resistance of cancer cells and increases the efficacy of the drugs on cancer patients. **SMR-36** showed potent inhibitory activity on both TOPO I and TOPO II, while **SBB** inhibited only TOPO I. Additionally, in silico molecular docking and molecular dynamics simulations were showed that **SMR-36** was interacted with the catalytic site of the topoisomerases, while, **SBB** bounded to both the catalytic side and one distinct side of the TOPO I. The binding site of the **SBB** could be targeted for drug development studies. Overall, all the findings suggested that **SMR-36** and **SBB** may be promising compounds as new anticancer agents. Also, the compounds might be further derivatized by *in silico* based analyses and be tested by more detailed cell-based and animal-based studies.

REFERENCES

Berendsen, H. J. C., Grigera, J. R., & Straatsma, T. P. (1987). The missing term in effective pair potentials. *Journal of Physical Chemistry*, 91(24), 6269–6271. Retrieved from https://doi.org/10.1021/j100308a038

Berman, H. M., Westbrook, J., Feng, Z., Gilliland, G., Bhat, T. N., Weissig, H., … Bourne, P. E. (2000). The Protein Data Bank. *Nucleic Acids Research*, 28(1), 235–242. Retrieved from https://doi.org/10.1093/NAR/28.1.235

Chen, S., Gomez, S. P., McCarley, D., & Mainwaring, M. G. (2002). Topotecan-induced topoisomerase IIα expression increases the sensitivity of the CML cell line K562 to subsequent etoposide plus mitoxantrone treatment. *Cancer Chemotherapy and Pharmacology*, 49(5), 347–355. Retrieved from https://doi.org/10.1007/s00280-002-0423-9

Choudhari, A. S., Mandave, P. C., Deshpande, M., Ranjekar, P., & Prakash, O. (2020). Phytochemicals in cancer treatment: From preclinical studies to clinical practice. *Frontiers in Pharmacology*, 10(January), 1–18. Retrieved from https://doi.org/10.3389/fphar.2019.01614

Darden, T., York, D., & Pedersen, L. (1993). Particle mesh Ewald: An N·log(N) method for Ewald sums in large systems. *The Journal of Chemical Physics*, 98(12), 10089–10092. Retrieved 22 May 2023 from https://doi.org/10.1063/1.464397

de Man, F. M., Goey, A. K. L., van Schaik, R. H. N., Mathijssen, R. H. J., & Bins, S. (2018). Individualization of Irinotecan Treatment: A Review of Pharmacokinetics, Pharmacodynamics, and Pharmacogenetics. *Clinical Pharmacokinetics*, 57(10), 1229. Retrieved 15 May 2023 from https://doi.org/10.1007/S40262-018-0644-7

Denny, W., & Baguley, B. (2005). Dual Topoisomerase I / II Inhibitors in Cancer Therapy. *Current Topics in Medicinal Chemistry*, 3(3), 339–353. Retrieved from https://doi.org/10.2174/1568026033452555

Emadi, A., Jones, R. J., & Brodsky, R. A. (2009). Cyclophosphamide and cancer: Golden anniversary. *Nature Reviews Clinical Oncology*, 6(11), 638–647. Retrieved from https://doi.org/10.1038/nrclinonc.2009.146

Ferlay, J., Colombet, M., Soerjomataram, I., Parkin, D. M., Piñeros, M., Znaor, A., & Bray, F. (2021). Cancer statistics for the year 2020: An overview. *International Journal of Cancer*, 149(4), 778–789. Retrieved 15 May 2023 from https://doi.org/10.1002/IJC.33588

Fisher, L. M., & Pan, X. S. (2008). Methods to assay inhibitors of DNA gyrase and topoisomerase IV activities. *Methods in Molecular Medicine*, 142, 11–23. Retrieved from https://doi.org/10.1007/978-1-59745-246-5_2

Grossman, S. A., Phuphanich, S., Lesser, G., Rozental, J., Grochow, L. B., Fisher, J., & Piantadosi, S. (2001). Toxicity, efficacy, and pharmacology of suramin in adults with recurrent high-grade gliomas. *Journal of Clinical Oncology*, 19(13), 3260–3266. Retrieved from https://doi.org/10.1200/JCO.2001.19.13.3260

Hess, B., Bekker, H., Berendsen, H. J. C., & Fraaije, J. G. E. M. (1997). LINCS: A Linear Constraint Solver for Molecular Simulations. *J Comput Chem*, 18, 14631472. Retrieved 22 May 2023 from https://doi.org/10.1002/(SICI)1096-987X(199709)18:12

Hockney, R. W., Goel, S. P., & Eastwood, J. W. (1974). Quiet high-resolution computer models of a plasma. *Journal of Computational Physics*, 14(2), 148–158.

Jurrus, E., Engel, D., Star, K., Monson, K., Brandi, J., Felberg, L. E., … Baker, N. A. (2018). Improvements to the APBS biomolecular solvation software suite. *Protein Science : A Publication of the Protein Society*, 27(1), 112. Retrieved 22 May 2023 from https://doi.org/10.1002/PRO.3280

Kim, S., Chen, J., Cheng, T., Gindulyte, A., He, J., He, S., … Bolton, E. E. (2023). PubChem 2023 update. *Nucleic Acids Research*, 51(D1), D1373–D1380. Retrieved 29 May 2023 from https://doi.org/10.1093/NAR/GKAC956

Krieger, E., & Vriend, G. (2002). Models@ Home: distributed computing in bioinformatics using a screensaver based approach. *Bioinformatics*, 18(2), 315–318.

Lapinskaite, R., Atalay Nazlıcan, H., Malatinec, Š., Donmez, S., Cinar, Z. O., Schwarz, P. F., … Rycek, L. (2023). Synthesis of Selagibenzophenone A and Its Derivatives for Evaluation of Their Antiproliferative, RORγ Inverse Agonistic, and Antimicrobial Effect**. *ChemistrySelect*, 8(7), e202204816. Retrieved 15 February 2023 from https://doi.org/10.1002/SLCT.202204816

Li, T. K., Houghton, P. J., Desai, S. D., Daroui, P., Liu, A. A., Hars, E. S., … Liu, L. F. (2003). Characterization of ARC-111 as a Novel Topoisomerase I-Targeting Anticancer Drug. *Cancer Research*, 63(23), 8400–8407.

Liew, S. K., Malagobadan, S., Arshad, N. M., & Nagoor, N. H. (2020). A Review of the Structure—Activity Relationship of Natural and Synthetic Antimetastatic Compounds. *Biomolecules*, 10(1). Retrieved 23 May 2023 from https://doi.org/10.3390/BIOM10010138

Lindahl, E., Hess, B., & van der Spoel, D. (2001). GROMACS 3.0: A package for molecular simulation and trajectory analysis. *Journal of Molecular Modeling*, 7(8), 306–317. Retrieved 22 May 2023 from https://doi.org/10.1007/S008940100045/METRICS

Liu, R., Zou, H., Zou, Z. X., Cheng, F., Yu, X., Xu, P. S., … Tan, G. S. (2020). Two new anthraquinone derivatives and one new triarylbenzophenone analog from Selaginella tamariscina. *Natural Product Research*, 34(19), 2709–2714. Retrieved 15 May 2023 from https://doi.org/10.1080/14786419.2018.1452008/SUPPL_FILE/GNPL_A_1452008_SM7795.PDF

Liu, X., Luo, H. Bin, Huang, Y. Y., Bao, J. M., Tang, G. H., Chen, Y. Y., … Yin, S. (2014). Selaginpulvilins A-D, new phosphodiesterase-4 inhibitors with an unprecedented skeleton from selaginella pulvinata. *Organic Letters*, 16(1), 282–285. Retrieved from https://doi.org/10.1021/ol403282f

Liu, X., Tang, G. H., Weng, H. Z., Zhang, J. S., Xu, Y. K., & Yin, S. (2018, December 2). A new selaginellin derivative and a new triarylbenzophenone analog from the whole plant of Selaginella pulvinata. *Journal of Asian Natural Products Research*. J Asian Nat Prod Res. Retrieved 31 May 2023 from https://doi.org/10.1080/10286020.2017.1378646

Martino, E., Della Volpe, S., Terribile, E., Benetti, E., Sakaj, M., Centamore, A., … Collina, S. (2017). The long story of camptothecin: From traditional medicine to drugs. *Bioorganic & Medicinal Chemistry Letters*, 27(4), 701–707. Retrieved from https://doi.org/10.1016/J.BMCL.2016.12.085

Miyamoto, S., & Kollman, P. A. (1992). Settle: An analytical version of the SHAKE and

RATTLE algorithm for rigid water models. *Journal of Computational Chemistry*, 13(8), 952–962. Retrieved 22 May 2023 from https://doi.org/10.1002/JCC.540130805

Nitiss, J. L. (2009). DNA topoisomerase II and its growing repertoire of biological functions. *Nature Reviews Cancer*, 9(5), 327–337. Retrieved from https://doi.org/10.1038/NRC2608

Okoro, C. O., & Fatoki, T. H. (2023). A Mini Review of Novel Topoisomerase II Inhibitors as Future Anticancer Agents. *International Journal of Molecular Sciences*, 24(3). Retrieved from https://doi.org/10.3390/ijms24032532

Pettersen, E. F., Goddard, T. D., Huang, C. C., Couch, G. S., Greenblatt, D. M., Meng, E. C., & Ferrin, T. E. (2004). UCSF Chimera--a visualization system for exploratory research and analysis. *Journal of Computational Chemistry*, 25(13), 1605–1612. Retrieved 29 May 2023 from https://doi.org/10.1002/JCC.20084

Ponder, J. W., & Case, D. A. (2003). Force Fields for Protein Simulations. *Advances in Protein Chemistry*, 66, 27–85. Retrieved from http://www.sciencedirect.com/science/article/pii/S006532330366002X

Skok, Ž., Zidar, N., Kikelj, D., & Ilaš, J. (2020). Dual Inhibitors of Human DNA Topoisomerase II and Other Cancer-Related Targets. *Journal of Medicinal Chemistry*, 63(3), 884–904. Retrieved from https://doi.org/10.1021/acs.jmedchem.9b00726

Tang, C. L., Alexov, E., Pyle, A. M., & Honig, B. (2007). Calculation of pKas in RNA: on the structural origins and functional roles of protonated nucleotides. *Journal of Molecular Biology*, 366(5), 1475–1496. Retrieved 29 May 2023 from https://doi.org/10.1016/J.JMB.2006.12.001

Trott, O., & Olson, A. J. (2010). AutoDock Vina: improving the speed and accuracy of docking with a new scoring function, efficient optimization and multithreading. *Journal of Computational Chemistry*, 31(2), 455. Retrieved 20 February 2022 from https://doi.org/10.1002/JCC.21334

Tumer, T. B., Yılmaz, B., Ozleyen, A., Kurt, B., Tok, T. T., Taskin, K. M., & Kulabas, S. S. (2018). GR24, a synthetic analog of Strigolactones, alleviates inflammation and promotes Nrf2 cytoprotective response: In vitro and in silico evidences. *Computational Biology and Chemistry*, 76(July), 179–190. Retrieved from

https://doi.org/10.1016/j.compbiolchem.2018.07.014

Vangone, A., Schaarschmidt, J., Koukos, P., Geng, C., Citro, N., Trellet, M. E., … Bonvin, A. M. J. J. (2019). Large-scale prediction of binding affinity in protein–small ligand complexes: the PRODIGY-LIG web server. *Bioinformatics*, 35(9), 1585–1587. Retrieved 21 March 2023 from https://doi.org/10.1093/BIOINFORMATICS/BTY816

Vos, S. M., Tretter, E. M., Schmidt, B. H., & Berger, J. M. (2011). All tangled up: how cells direct, manage and exploit topoisomerase function. *Nature Reviews. Molecular Cell Biology*, 12(12), 827. Retrieved 20 February 2022 from https://doi.org/10.1038/NRM3228

Wang, C. G., Yao, W. N., Zhang, B., Hua, J., Liang, D., & Wang, H. S. (2018). Lung cancer and matrix metalloproteinases inhibitors of polyphenols from Selaginella tamariscina with suppression activity of migration. *Bioorganic & Medicinal Chemistry Letters*, 28(14), 2413–2417. Retrieved from https://doi.org/10.1016/J.BMCL.2018.06.024

Yin, D., Li, J., Lei, X., Liu, Y., Yang, Z., & Chen, K. (2014). Antiviral activity of total flavonoid extracts from selaginella moellendorffii hieron against coxsackie virus B3 in vitro and in vivo. *Evidence-Based Complementary and Alternative Medicine*, 2014. Retrieved from https://doi.org/10.1155/2014/950817

APPENDIX

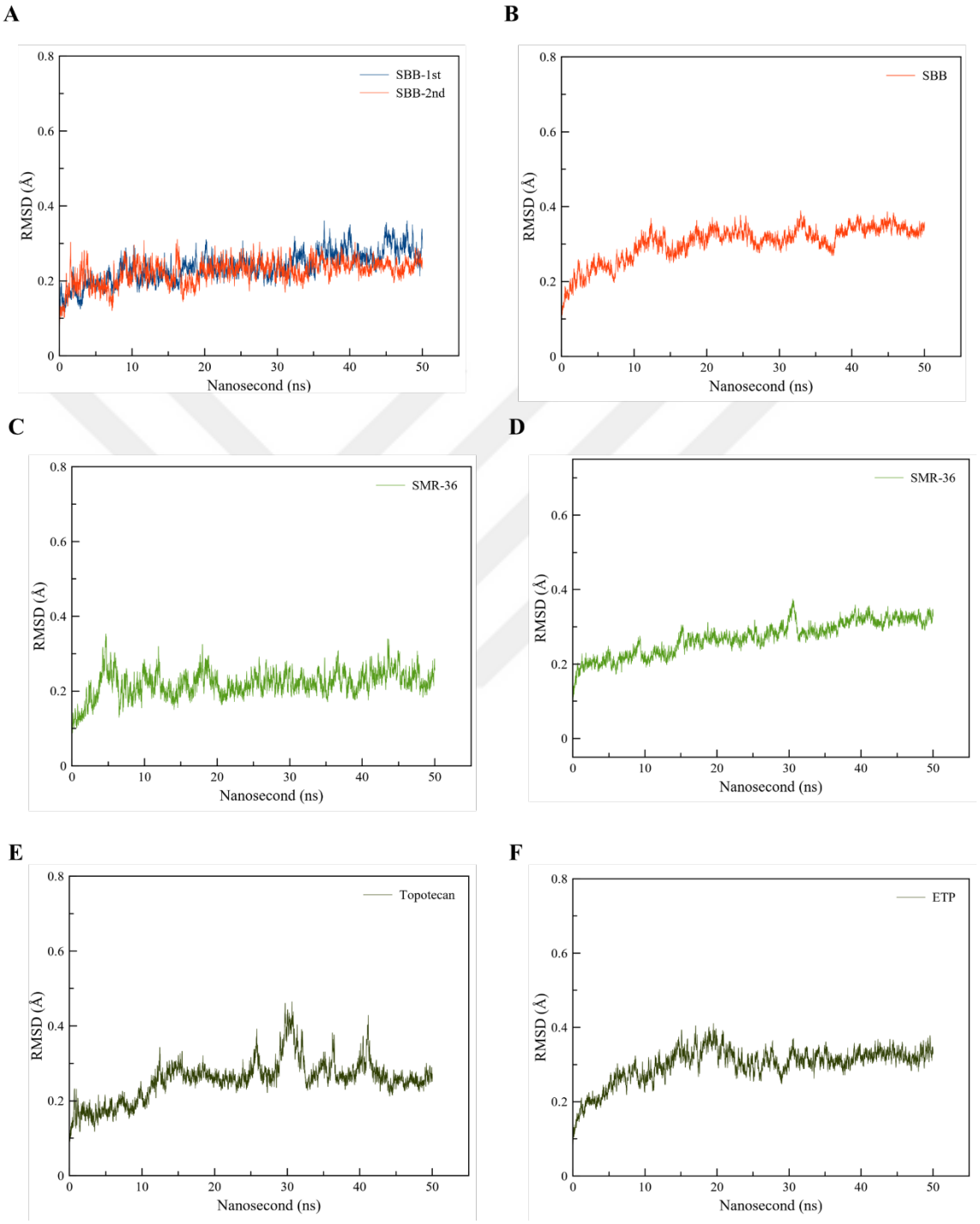

Figure 1. RMSD values of Topoisomerase I (A,C,E) and II (B,D,F) at the end of the protein-ligand MD simulations.

BIOGRAPHY